nature portfolio

Peer Review File

Inhibition of host N-myristoylation compromises the infectivity of SARS-CoV-2 due to Golgi-bypassing egress

Corresponding Author: Dr Merja Joensuu

This file contains all reviewer reports in order by version, followed by all author rebuttals in order by version.

Version 0:

Reviewer comments:

Reviewer #1

(Remarks to the Author)
Summary
In this manuscript, Saber et al. propose the enzymes N-myristoyltransferases as a potential antiviral target against SARS-CoV-2 and RSV viruses. The authors make a significant effort to elucidate the mechanism behind the viral inhibition, revealing that the inhibitor IMP-1088 specifically acts during the late stage of SARS-CoV-2 replication. This drug impairs the maturation of the newly synthetized viral particles and disrupt the conventional egress. The authors described that this effect is due to an alteration of the secretory pathway membrane trafficking following IMP-1088 treatments. Mechanistic studies were conducted in one cell line (A549-AT cells), while the antiviral effect was also evaluated in human lung and nasal epithelial cells, as well as human choroid plexus brain organoids (ChPCOs). Regarding the latter, in the current stage the data obtained using the ChPCOs organoid are rather prelimary and do not provide additional insights. Therefore, the authors would be advised to consider removing these data from the manuscript.
Overall, the manuscript is well-written, with clear figures and contain detailed experiments into the mechanistic effect of how IMP-1088 may influence SARS-CoV-2 infection. However, there are some changes that could further strengthen the manuscript:

Major critiques:
1. Fig 1H-J: the authors concludes that IMP-1088 does not inhibit the viral entry. To further assess this, the authors should perform qRT-PCR on SARS-CoV-2 on cell lysate and supernatants to exclude that the treatments does not affect viral replication.
2. Fig 1: overall the authors performed viral entry and replication assay using only one cell line. It would be interesting to include another cell line (such CALU-3 cells) as a cellular model to mimic SARS-CoV-2 infection of human lung cells.
3. Fig 1Q: 'SFV-GFP and VSV-GFP infections, on the other hand, were not affected by the drug treatment at 12 hpi (MOI 0.5), or 24 hpi (MOI 0.01)'. What is the rational or based on what data were these two different MOIs at the two different time points decided on?
4. Fig 2: overall, the results on ChPCOs organoids are currently preliminary and, in part, in contrast to the existing literature. In this model the authors showed SARS-CoV-2 infection of MAP2+ neuronal cells. However, it has previously been demonstrated that cortical neurons are not permissive to the infection and only <0.1% of neurons are infected by SARS-CoV-2 (PMID: 32579880; PMID: 33010822). Therefore, a more pure choroid plexus (ChP) model (PMID: 33010822; PMID: 33113348), quantifying infection (N protein) on ChP TTR+ cells, would be more appropriate for the question that the authors wish to address
5. Fig 2: the data shown, as far as one can conclude from the legend, are based on a single biological replicate and just two technical replicates. This is insufficient for stem cell based-disease modelling. The current ISSCR guidelines recommend the use of three hPSC/iPSC lines for stem cell studies. Furthermore, independent differentiation experiments (at least three biological replicates) are required to support the claims.
6. Fig 2: Moreover, it is unclear how the authors segmented the MAP2+ staining. It is not clear that MAP2 staining can accurately be segmented into individual neurons (if successful, such a segementation strategy should be shown in the supplementary figures). If this is the goal (and one could argue that indeed one should not be interested in neurons but rather ChP cells), one could better segment individual nuclei using a marker such as HuC/HuD.
7. Fig 2: the authors provided the quantification of cleaved Caspase-3. Please show representative ICC images for these stainings.
8. In summary, the data in Fig 2 and in Supplementary figures 2, 3 and 4 do not add further value to the manuscript, and as

such the authors should consider removing these data.
9. 'We observed significantly decreased levels of infection caused by virions released from IMP-1088-treated cells compared to those released from DMSO-treated cells (Figs. 2I-J)'. At which time points were the supernatants from infected cells collected? Has the amount of SARS-CoV-2 been added to the organoids at equal amount? Please provide more experimental details.
10. Fig 3 A-B: the qRT-PCR results showed at the different time point from 0 up to 48h hpi should be included in a single plot using the same axes.
11. 'In contrast, analysis of the S protein, which is key to the viral infectivity, indicated that virions released from IMP-1088-treated cells contained significantly less total S protein..'. In Fig 3F, it is not clear whether the western blot has been performed from cell lysate or supernatants. The authors claim that the virion released has less S cleaved protein. To this aim, the virus should be collected from the supernatants and purified by ultracentrifugation and the western blot should be performed on the purified viral particles.
12. For Fig 4, while providing interesting leads on how NMT inhibition in the host may affect virion infectiousness, the data would be better combined with the experimental data in Fig 5 which validate the key pathways that are perturbed by IMP-1088 treatment.
13. Fig 5: Considering how IMP-1088 affects A549-AT cells and the magnitude of the phenotypes seen in the ERGIC and Golgi apparatus, the authors should validate these findings in the disease-relevant models used in Fig 1 (e.g. nasal epithelium and human lung) for both the ERGIC-53 stainings, the GM130 stainings, and importantly test for cytotoxicity in all models used (this also considering the changes in Actin staining seen in Fig 6).
14. 'Unexpectedly, in IMP-1088 treated cells, we also observed the release of virions from structures resembling ER (Fig. 7D). In support, electron tomography (ET) analysis revealed small opening from ER to the plasma membrane (Fig. 7E).' In Fig 7D seems that the treatment of IMP-1088 increases the number of vesicles. Have the authors quantified whether the number of vesicles is higher in treated cells compared to DMSO? Can the authors further investigate if the virus is trapped within these vesicles?
Minor critiques:
1. Fig 1D: the authors showed that the inhibition of N-myristoyltransferases reduces the formation of syncytia formation. Please provide quantification of these data.
2. Fig 3C: the images do not represent the graph, although the quantification show a reduction of N protein compared to the DMSO treated cells, the staining of N protein in Wash- condition in IMP-1088 treated cells is higher compared to the non-wash condition. Please provide representative and high-quality images (perhaps these were lost with PDF compression).
3. There is an error in the correspondence of the letters between the text and the figures: (Fig 5F, G) is the 5H, 5I. (Fig 5H) is 5L. (Fig 5H) is 5L. Fig 5J is 5N.
4. There are some minor typo's throughout the manuscript. Please address these and if possible add line numbers to easily identify such errors.

Reviewer #2

(Remarks to the Author)
I co-reviewed this manuscript with one of the reviewers who provided the listed reports. This is part of the Nature Communications initiative to facilitate training in peer review and to provide appropriate recognition for Early Career Researchers who co-review manuscripts.

Reviewer #3

(Remarks to the Author)

This manuscript reports an interesting observation that NMTs inhibitor IMP-1088 displayed very robust inhibition effects on the assembly and/or release of SARS-CoV-2 in cell lines, in primary human nasal epithelial cells, and in brain organoids, which was due to disruption of conventional secretory pathway and activation of Golgi-bypassing lysosomal exocytosis. IMP-1088 also inhibits RSV infection, probably by a similar mechanism.
Overall, the conclusions will be interesting to the field and a number of experiments and volume of data are presented. However, the conclusion is not strongly supported. Most experiments are based on the inhibitor IMP-1088 treatment and manipulation of NMTs protein is missing. Also, validation of the identify of key protein or proteins downstream of the NMTs, whose N-myristoylation is required for SARS-CoV-2 assembly, is lacking. For some results, additional detail and explanation would be helpful. The following concerns need to be addressed before considering acceptance for publishing in Nature Communications.

Specific major comments:

1. Previous study showed that N-myristoyltransferase 1 is essential for mice embryo development but is not essential for cell lines, and NMT-1 knockout cells displayed 95% reduction of the NMT activity. NMT-1 knockout or knockdown (if not NMT1/NMT2 together) should be performed to test its effect on SARS-CoV-2 assembly and secretion.

2. IMP-1088 treatment did not display inhibitory effects on the viral RNA release at 12 hpi. At 12 hpi, does IMP-1088 treatment reduce the viral infectivity of release viruses? Also, at 12 hpi, does IMP-1088 treatment reduce viral protein (S, M) levels in media by WB? This is an important question since multiple rounds of infection will make the results very difficult to interpret. One replication cycle for SARS-CoV from absorption to release of infectious virions is about 7-8 hours, which is probably the similar case for SARS-CoV-2. To test the viral infectivity of release virions, released viral RNA amount, and released viral protein levels, with and without IMP-1088 treatment, in one but shorter than two SARS-CoV-2 replication

cycles, is highly recommended to strengthen the manuscript's conclusion.

3. In Figures 3F and 3H, what about the S and M protein blots in the cell lysates? It will be more convincing if these assays could be done for a short infection time (from 1 to shorter than 2 cycles).

4. An intracellular viral titer assay (measuring the viral infectivity of virions inside the cells) is required to confirm that IMP-1088 treatment indeed disrupts SARS-CoV-2 assembly and produces less infectious virions. It will be good to perform it for a short time of infection (shorter than 2 replication cycles).

5. For the cellular viability assay, A549-AT cells treated with IMP-1088 and infected by SARS-CoV-2 should be tested. It is possible that IMP-1088 treatment alone does not cause cell death, but the combination of IMP-1088 treatment and SARS-CoV-2 infection induces a significantly higher cell death rate than SARS-CoV-2 infection alone.

6. It is an interesting observation that among 4 viruses that do not have N-myristoylation viral proteins, NMTs inhibitor selectively inhibits SARS-CoV-2 and RSV, but not SFV and VSV, although all these 4 viruses are enveloped single-stranded RNA viruses. SFV, VSV, and RSV are assembled at the host cell plasma membrane, but NMTs inhibitor only inhibits RSV but not the other two. More comments on this will be good.

7. The authors hypothesized that IMP-1088 treatment disrupted the secretory pathway and activated an alternative SARS-CoV-2 egress pathway which bypassed the Golgi apparatus, but lysosomal exocytosis of SARS-CoV-2 without any NMTs inhibitor treatment was proposed in reference 11, 12, 52, etc. Are the authors arguing that under normal conditions, SARS-CoV-2 exits the host cells via the conventional secretion pathway?

Specific minor comments:

1. It is very surprisingly impressive that 1-minute IMP-1088 treatment is as robust as 48-hour treatment in inhibiting the infection rate. It will be interesting and strengthen the authors' conclusion to test the effects of 1-minute IMP-1088 treatment on SARS-CoV-2 assembly, secretion, ER and Golgi structure. N-myristoylation is an irreversible modification. One-minute treatment may efficiently block the myristoylation of nascent proteins but not existing proteins. How can one-minute treatment displays such a robust inhibition of viral infection needs more explanation and discussion.

2. For the virus entry assay (Figure 1H-J), a more detailed description (for example, MOI, and whether viruses are washout) or method is needed. Also, 8 h infection is a little bit long. The virus entry assay in this study (PMCID: PMC10130743) is well-performed and more convincing.

3. For EM imaging, 48 h infection is a little bit too long. The shorter the time of infection, the better for observing the subcellular ultrastructure dynamics. For example, in Figure 6B, viral particles were notably absent in the ERGIC and Golgi apparatus of IMP-1088 treated cells, which was likely due to the lower infection in IMP-1088 treated cells at 48 hpi.

4. It was reported that SARS-CoV-2 mediated Golgi fragmentation accelerated viral assembly and trafficking. Can authors make some comments on it?

5. Both references 72 and 73 referred to VSV assembly, and the SFV assembly citation was missing.

6. On page 9, Hela should be HeLa, reference 19 was put inside the word.

7. On page 7, We was written as Wwe.

Reviewer #4

(Remarks to the Author)
Overall, this is a well designed and reported study with some significant potential impact on human health as it relates to some viral infections. The rationale is sound, results support the major conclusions and the manuscript is written well. While using the organoid-derieved approach to increase human disease relevance and human donor nasal cells were included, the relevance of these "artificial" growth lacking full human microenvironment is still a concern, although one that may be limited to overcome. Validation of the findings in animal models is lacking and would be the next step to more fully characterize the mechanisms in a fully competent microenvironment model, specifically to understand the impact of NMT inhibition on normal homeostasis. Specifically, how will non-infected cells or other cells systemically be impacted by inhibition of NMTs. Also, using genetic perturbations (CRISPR/RNAi) to validated the drug activity vs off-target effects driving the phenotype would be important. Overall, this is a well rounded study with very interesting conclusions. Minor comments: figure 4 resolution is lower than ideal.

Reviewer #5

(Remarks to the Author)
The manuscript titled "Inhibition of host N-myristoylation compromises the infectivity of SARS-CoV-2 due to Golgi-bypassing

egress from lysosomes and endoplasmic reticulum“ by Saber et al. presents data on the antiviral activity of IMP-1088, an inhibitor of cellular N-myristoyltransferases (NMT), and investigates the mechanisms of action in an infection by a virus without known myristoylation sites, which is a relevant extension to previously published work on NMT inhibitors in viral infections (Mousnier et al., Nat Chem. 2018).
The research offers interesting insights into a potential new therapeutic option for specific viral infections, including Sars-CoV-2 and RSV. Overall, the manuscript is well-written, and the presentation of the results is largely comprehensive. Nevertheless, there are certain shortcomings that should be addressed. I have provided my comments and suggestions below.
I hope my comments will be helpful in revising the manuscript. I am confident that with these revisions, the paper will make a valuable contribution to the field, and I recommend accepting the manuscript with major revisions addressing the comments below.

Major Comments:
1. The authors present an extensive dataset investigating the therapeutic potential of NMT inhibition. However, the study focuses solely on in vitro experiments and cellular models and lacks a discussion on the pharmaceutical usability of NMT inhibitors and potential adverse side effects. Although in vivo testing of NMT inhibitors may not be within the scope of this study, the manuscript would benefit from a discussion of the limitations of the cell lines, in vitro models, and organoid systems employed. This would provide valuable context to the reader and help to evaluate the translational potential of the findings.
2. Page 3 “Our findings demonstrate that inhibiting NMT1 and NMT-2 in human lung and primary nasal epithelial cells, as well as in human 3D choroid plexus-cortical neuron organoids, disrupts viral assembly and maturation by interfering with the host cell's secretory pathway membrane trafficking.” The authors state here that they show effects in “human lung […cells]”. The model they use are “human lung small carcinoma cells that were engineered to stably express the virus receptor ACE2 and protease TMPRSS2, […]”. Please indicate that the experiments were done using a cancer cell line and not primary human lung specimen.
3. Figure 2 A/B, as well as Suppl Figure 2 and 3, show the scRNA-seq data of the ChPCOs as UMAP representations and the expression of key genes as feature plots. These plots are hard to read and give little quantitative information about the gene expression per cluster. As shown in Suppl. Fig 4, visualization of the gene expression per cell type as violin plots or a dot plot allows to understand the number of cells expressing the gene and the relative average expression level of the gene much better. Specifically, ACE2 and TMPRRS2 seem to be detected only in very few cells. Using a dotplot, the expression of all genes shown in Figure 2 and Suppl. Figures 2, 3 and 4, could be easily summarized in a single figure giving a much simpler, yet more comprehensive and informative visualization of genes expression in the main figure 2.
4. Page 7: “In addition, Wwe also quantified the level of SARS-CoV-2 infection in ChPCOs using virions released from either DMSO or IMP-1088-treated cells (Fig. 2E).” Please specify in which cells these virions were produced.
5. In the single cell RNA-seq data of ChPCOs, what is the expression level of NMT1 and NMT2? Which cells, if any, show a high expression?
6. According to the “Data and Code Availability” section, the authors do not intend to publish the code used for the transcriptomics analysis. I strongly recommend publication of the code for the community to have a chance to reproduce and evaluate the analyses performed in this study. This is currently not possible and hampers the evaluation of the manuscript.
7. Please clarify if the ChPCOs used in this study were derived from multiple donors or all from a single donor?
8. The presentation of the single-cell RNA-seq data does not allow to evaluate the cell type annotation. Please include a dot plot of all marker genes determined using the FindAllMarkers function and used for cell type annotation in the supplementary figures as described in the methods section under “scRNA-seq analysis”.
9. The access token provided for the review of the GEO submission is not working. Please check if the token is correct and still valid.
10. Page 8: “Following our findings of host cell NMT inhibition leading to a significant decrease in infectivity of the released virions and the perturbed trafficking of the viral particles to ERGIC and Golgi compartments, we next explored the potential impact of this transport blockage on the structural proteins of the released virions.” The perturbed trafficking of the viral particles to ERGIC and Golgi has not been shown at this point in the manuscript.
11. Page 8 “We observed slightly decreased levels of the viral N protein, which is important for viral genome packaging, in virions released from both DMSO and IMP-1088-treated cells (Figs. 3F, 3G).“ Slightly decreased in comparison to what?
12. Page 9: “The inhibition of cellular NMT led to significant changes in the abundance of proteins across multiple subcellular pathways (Fig. 4A), particularly those involved in the early secretory pathway endoplasmic reticulum (ER), ER-Golgi intermediate compartment (ERGIC), and Golgi apparatus and vesicle trafficking (Figs. 4B).” Please discuss potential adverse side effects of this fundamental effect on the proteome?
13. Page 9, “NMTs regulate protein homeostasis”. Please specify in the main text how the Gene Set enrichment analysis was performed and which annotation data base was used.
14. Page 9, “Further analysis revealed a significant decrease in the abundance of proteins with N-terminal glycine destined for N-myristoylation (Fig. 4C).” Please extend the description of this figure and explain the analyses and comparisons done here to published data.
15. Page 10 “A treatment with 5 µg/mL BFA for 40 s or 4 min led to a loss of the Golgi localization and to a homogenous distribution throughout the cell (Fig. S6A,B). These effects were different from IMP-1088, where we discovered that the treatment with 1 µM IMP-1088 for 1h or 48 h induced a gradual dispersal and fragmentation of Arf1-GFP signal (Fig. S6C; Note the considerably longer treatment), supporting previous findings that NMT inhibition blocks coatomer complex I (COPI) assembly and results in Golgi dispersal51. We observed a gradual increase in the mean fluorescence intensity (Fig. S6D), along with decrease in the mean spot size (Fig. S6E), and an increase in the number of spots
(Fig. S6F), of ARF1-GFP following IMP-1088 treatment. Together, these results indicate that the effects of IMP-1088 to the secretory pathway organelle morphology and trafficking are different from BFA, which is a well-established inhibitor of ARF1.” The authors specifically mention the considerably different treatment times. How are these findings comparable?

16. The manuscript has no information or discussion on the potential application of NMT inhibitors in humans and adverse side effects. Please include these topics in the discussion and elaborate on the pharmaceutical use of such drugs.
17. Line numbering would have been very helpful for the reviewing process. Please include line numbers in any future versions of this manuscript.

Minor comments:
1. Fig. 1R: the x-axis ticks are off.
2. Fig. 2A: “umap_3” on y axis.
3. Fig. 2C: I do not understand why the UMAP in Fig 2C is its own panel compared to the UMAPs shown in Fig. 2B.
4. Page 7: “Compared to control organoids treated only with vehicle (DMSO), those ChPCOs treated with IMP-1088 or Apilimod exhibited significantly reduction in fewer SARS-CoV-2 infected cells (Figs. 2D, 2F).” I think the wording needs to be corrected here. A “reduction in fewer infected cells” sounds like an increase to me.
5. Page 7: “In addition, Wwe also quantified the level of SARS-CoV-2 infection in ChPCOs using virions released from either DMSO or IMP-1088-treated cells (Fig. 2E).” Please correct the typo.
6. Suppl. Figure Legends refer to the organoids as CPCOs, whereas they are called ChCPOs in the test. Please unify the annotation.
7. Methods section (Page 7 of supplemental information): “Double
detection was performed to …” Please correct the typo (“Doublet”).
8. Page 9: “Following the findings of the mass sp 19ectrometry analysis”. Please correct the positioning of the reference.
9. Page 10: “N-myristoylation is a conserved feature of ARFs, including ARF147. To characterize the effects of IMP-1088 treatment on secretory pathway trafficking further, we next compared the of IMP-1088 treatment to Brefeldin-A (BFA), which is an ADP-ribosylation factor 1 (ARF1) inhibitor …” Please introduce the ARF abbreviation when using it for the first time.

Reviewer #6

(Remarks to the Author)
The manuscript of Saber et al. focusses on the activity of IMP-1088, a drug that inhibits cellular N-myristoylation and was shown to have antiviral potential on Rhinoviruses. The drug is shown to inhibit SARS-CoV-2 infectivity by disrupting viral assembly and maturation thus releasing virions with compromised infectivity. The hypothesis put forward is that incomplete maturation in IMP-1088 treated cells is due to lack of Furin cleavage because virions are diverted from ERGIC/Golgi where Furin resides to lysosomes/plasma membrane. If the purpose of the manuscript is to describe the mode of action of an antiviral drug first would be necessary to convince the reader that the drug could be potentially effective in vivo. Cellular models of infection included A549-AT cells, nasal epithelial cells and human 3D choroid plexus-cortical neuron organoids. However, cytotoxicity was measured only for A549-AT and also incompletely. Furthermore, the drug, which is almost an irreversible inhibitor of N-myristoylation, may impact essential activities that may not appear in a cytotoxicity assay in cell culture. Hence, the data provided so far are not yet sufficient to put too much emphasis on antiviral development. Some experiments such as: (lack of) inhibition of other viruses, scRNAseq, proteomic analysis are poorly contextualized in the logic frame of the work. The manuscript is written sometimes in a disordered way in the flow of experiments and would need to be better structured. The final model of altered secretion requires more evidence.
Specific comments:
Virus inhibition in A549-AT cells shows 50% efficacy at 24hpi and better effect at 48hpi (except for Omicron that remains at 50% inhibition also at 48hpi). Being such a potent inhibitor why it takes so much time for complete inhibition? In 24 you may have reconstitution of HMT activity from neo-synthesized protein.
Cytotoxicity assay in A549-AT cells is not complete, it stops at 1 uM with already signs of toxic effect. A complete CC50 and EC50 profile with selective index would be welcome both at 24/48 hpi with the same protocol of exposure to the drug.
A complete ToA experiment with addition of the drug at timepoints after infection and a virucidal activity on the virion would be a more comprehensive testing of an antiviral drug.
Not clear the meaning sequencing the virus just after treatment, usually virus that overcomes drug inhibition is sequenced after passaging several times under drug selection. Here seems to be 24-48hpi, not clear, Table 1 is missing?
The experiment at 8hpi figs 1H-j could be interpreted differently, being a drug acting fast on the cellular HMT enzyme but exerting its antiviral effect slow requiring 48-72h.
Nasal cells from human donors are quite heterogeneous depending on various factors including age, how many different donors per experiment?
The experiment in nasal cells lead to a statement of defect in spread of the NMT inhibition without actual evidence of it, which comes later on in the text.
Testing different viruses would be useful to check for specificity of treatment and eventually to classify mechanism based on similar action. However, from the text it is not clear why they are doing this testing. What is the discriminant among these 4 viruses? Needs explanation/clarification. Furthermore Fig 1 PQR show 2 conditions 1 or 2 hbi pretreatment with drug and 24 or 48 hpi test of infection, what is the rationale? Not really comparable.
Is choroid plexus the right model to use? Neuronal infection of SARS-CoV-2 is highly debated and need to be more cautious on this. A model based on pulmonary cells would have been safer.
Concerning choroid plexus scRNA data, what is the relative composition of cell types infected by CoV2, need to show viral transcripts in the graph – here they also start to talk about decreased infectivity of released virions. This is reinforced in the next paragraph measuring infectivity of released virus.
Page 8 – they state that “Following our findings of host cell NMT inhibition leading to a significant decrease in infectivity of the released virions and the perturbed trafficking of the viral particles to ERGIC and Golgi compartments, we next explored ….” Where is the evidence? Again it comes later in the text.

Figure 3 (F) Western blot of uncleaved viral spike (S) ± glycosylation? Where is the evidence of glycosylation? Don't see different migration of bands.
The mass spec data show info on perturbation of myroistilated proteins by the inhibitor. Some discussion would be required on other pathways such as activation of ER Stress pathways that could contribute to inhibitory phenotype.
Electron microscopy shows gross rearrangement of membranes, IF shows disruption of ERGIC. Immunostain shows disruption again. All descriptive. All this part is in sterile conditions and related to the function of the inhibitor. Functional data follow with ARF-GFP again in sterile conditions. Any data in infection?
Furin comes up as surprise next. What I the rationale?
Fig 7A – seems that treatment did not decrease infectivity comparing the two graphs, but maybe two dfferent dataset, explain.
Final chapter deals wit the Spike secretion using ectopic expression of S-wt, but the construct is not well described, is it full Spike with TM or w/o? Ancestral seq?
What means "immunostained against internal (magenta) and secreted (green) Swt"
"
Last part rather confused an needs clarification. The conclusion that defect virus maturation in treated cells is due to lack of Furin cleavage because virions are diverted from ERGIC/Golgi where Furin resides to lysosomes/plasma membrane is poorly supported by the data. Pathway of ectopic Spike may well be different from virion. Would it be possible to rescue inhibition by targeting Furin to this undescribed secretion pathway? Here there is need of more supporting evidence.

Version 1:

Reviewer comments:

Reviewer #1

(Remarks to the Author)
In the current version of the manuscript, Saber et al have addressed most, if not all, of the major comments suggested by the reviewers. The authors have improved the overall clarity of the manuscript and more clearly described the figures in the legends. While the hPSC-derived ChPCO experiments now adhere to ISSCR guidelines (using three independent hPSC lines), whether the ChPCO model is the most relevant model for this particular study is questionable. As SARS-CoV-2-induced encephalitis is highly rare and the IMP-1088 experiments rely on pre-treatment of ChPCOs, their translational potential remains unclear. However, the data on the antiviral activity of IMP-1088 and its mode of action are of interest to both the SARS-CoV-2 and broader virology field.

Reviewer #2

(Remarks to the Author)
I co-reviewed this manuscript with one of the reviewers who provided the listed reports. This is part of the Nature Communications initiative to facilitate training in peer review and to provide appropriate recognition for Early Career Researchers who co-review manuscripts.

Reviewer #3

(Remarks to the Author)
The revised manuscript is improved by adding new results and rephrasing the text. However, the conclusions, especially the hypothesis (in the abstract) that "NMT1 inhibition triggers a novel Golgi-bypassing pathway for SARS-CoV-2 progeny virion egress", are not fully supported. The authors also stated in the review response letter that " Based on the current understanding of Coronavirus assembly and egress, the virions are believed to reach the Golgi compartment where the viral E, M, spike must be glycosylated and, in the case of SARS-CoV-2, the spike is cleaved by furin. From the Golgi compartment a transport mechanism to the lysosomes has been proposed, which in turn results in delivery of mature virions to secretory lysosomal vesicles that have a neutral pH" Please list the references (research articles, since many reviews proposed various pathways) supporting the Golgi to lysosome egress pathways of SARS-CoV-2. In contrast, it is widely accepted that SARS-CoV-2 undergoes a Golgi-bypass unconventional pathway for release, which was first proposed in 2020 (PMID:33157038) and strengthened by different groups (PMID:33422265; PMID: 36563151; PMID:34995113). Recently, two different teams reported that BFA treatment inhibits SARS-CoV-2 assembly and secretion (PMID: 40540531; PMID: 40634337), which suggests ER to Golgi pathway is important for SARS-CoV-2 assembly/trafficking and challenges the Golgi-bypassing egress pathway. Therefore, the authors prefer Golgi-bypassing pathway for SARS-CoV-2 release, and it is not novel but a more widely accepted model. The authors should make it clearer about the SARS-CoV-2 egress pathway under normal conditions and under N-myristoylation inhibition.
The authors reasoned that " To our knowledge, isolation of SARS-CoV-2 intracellular and intact virions is, thus, not feasible." For example, in the paper mentioned above (PMID: 40540530), intracellular virion titer was measured for a short period of SARS-CoV-2 infection. Also, WB for released virions was done after PEG enrichment, not supporting "WB could not be performed at this early time point (12 hpi)".
In Figure 7C, in addition to Spike and LAMP1 colocalization analysis, co-staining of Spike and a Golgi marker would be strong evidence to support the authors' conclusion.
In the paper (PMID: 40634337), Arf1 plays an important role in SARS-CoV-2 assembly by directly interacting and facilitating the ERGIC accumulation of M protein. As loss of N-myristoylation in Arf1 disrupts its Golgi membrane association, and 1 uM

IMP1088 treatment did not significantly alter Arf1 Golgi association, more discussion will be valuable.

Reviewer #5

(Remarks to the Author)
Overall, I applaud the authors for adding a considerable amount of new data to address the majority of my previous comments in a satisfactory manner, and I acknowledge that the manuscript has improved as a result of the revisions. I appreciate the effort made to clarify various aspects of the work.

That said, I would like to raise a general concern about the review process. I had the impression that the authors did not take sufficient steps to facilitate the reviewers' task. Most notably, the absence of tracked or highlighted changes in the revised manuscript made it unnecessarily difficult to assess what had been modified. While the authors added line numbers, they only used them to refer to changes in some answers. This added considerable effort to the re-evaluation and, in my view, does not align with best practices in scientific communication.

In addition, my specific request for a GEO accession number was not adequately addressed. Although the authors mention that this information was provided to the editor, I did not receive it. Accessing such essential data should not be this cumbersome, particularly when it is necessary for a proper and complete review.

Finally, I found that the presentation of certain materials—especially Table 3, which lists the top 50 marker genes per cell type—still requires improvement. In its current format, the table is not particularly readable, which diminishes its utility. A dot plot, as I previously suggested, would have been a much more effective and accessible way to present this information.

Nevertheless, I am convinced the paper will make a valuable contribution to the field, and I recommend accepting the manuscript for publication.

Additional minor comments:

Line 76/77: "of" is missing.

Reviewer #6

(Remarks to the Author)
I'm happy with the rebuttal of the authors, manuscript is improved and could be published, no further comments.

REVIEWER COMMENTS

Reviewer #1 (Remarks to the Author):

Summary
In this manuscript, Saber et al. propose the enzymes N-myristoyltransferases as a potential antiviral target against SARS-CoV-2 and RSV viruses. The authors make a significant effort to elucidate the mechanism behind the viral inhibition, revealing that the inhibitor IMP-1088 specifically acts during the late stage of SARS-CoV-2 replication. This drug impairs the maturation of the newly synthetized viral particles and disrupt the conventional egress. The authors described that this effect is due to an alteration of the secretory pathway membrane trafficking following IMP-1088 treatments. Mechanistic studies were conducted in one cell line (A549-AT cells), while the antiviral effect was also evaluated in human lung and nasal epithelial cells, as well as human choroid plexus brain organoids (ChPCOs). Regarding the latter, in the current stage the data obtained using the ChPCOs organoid are rather prelimary and do not provide additional insights. Therefore, the authors would be advised to consider removing these data from the manuscript.
Overall, the manuscript is well-written, with clear figures and contain detailed experiments into the mechanistic effect of how IMP-1088 may influence SARS-CoV-2 infection. However, there are some changes that could further strengthen the manuscript:

Major critiques:

1. Fig 1H-J: the authors concludes that IMP-1088 does not inhibit the viral entry. To further assess this, the authors should perform qRT-PCR on SARS-CoV-2 on cell lysate and supernatants to exclude that the treatments does not affect viral replication.
We thank the reviewer for this comment, which enabled us to further refine the antiviral mechanism. As suggested, we performed qRT-PCR on cell lysates from SARS-CoV-2-infected cells, complementing the previously shown qRT-PCR data from released virions in the culture supernatant (old Fig. 3A, B). IMP1088 was added at 1.5 hbi, and cell lysates were collected at 0, 6, 12, 24, and 48 hpi. The new qRT-PCR results from cell lysates and supernatants are now shown in Fig. 4H and 4J, respectively. These data demonstrate that IMP-1088 delays viral replication kinetics by 8 hpi (Fig. 4H), while a significant reduction in viral egress is only observed from 24 hpi onward (Fig. 4J).

2. Fig 1: overall the authors performed viral entry and replication assay using only one cell line. It would be interesting to include another cell line (such CALU-3 cells) as a cellular model to mimic SARS-CoV-2 infection of human lung cells.
As suggested by the reviewer, we have now included experiments on Calu-3 cells. In the new Fig. 1H–J, we show that IMP1088 treatment at 24 hbi significantly reduces SARS-CoV-2 infection in these human lung cells. In contrast, treatment at 1 hbi does not significantly reduce infection, although a decreasing trend is observed (Fig. 1J).

3. Fig 1Q: ‘SFV-GFP and VSV-GFP infections, on the other hand, were not affected by the drug treatment at 12 hpi (MOI 0.5), or 24 hpi (MOI 0.01)’. What is the rational or based on what data were these two different MOIs at the two different time points decided on?
We thank the reviewer for this comment and have addressed the MOI question with new experiments. Viral replication kinetics vary by virus and cell type: VSV and SFV replicate rapidly (up to 10^9 infectious units/mL within 20 h), while SARS-CoV-2 and RSV replicate more slowly (10^6 infectious units/mL in 48 h).

We performed extensive dilution series for each virus and selected MOIs that yielded comparable infection levels at 24 hpi (Fig. 1P). Note that SFV infection appears as GFP-positive puncta, whereas VSV infection results in uniform cytoplasmic GFP expression. To better compare the effects of IMP1088, we repeated the VSV and SFV infection experiments using MOI 0.001, which allows multiple rounds of infection over the 24-h experimental period. A549 cells were pre-treated with IMP1088 either 1 h or 24 h prior to infection and fixed after 24 h (extending infection to 48 h results in extensive cell death and detachment).

Unlike our earlier experiments with higher MOIs, the new data show that IMP1088-treatment 24 h prior to infection significantly inhibited VSV, but not SFV (Fig. 1R and 1S, respectively). While further studies are needed to understand why SFV is unaffected, we speculate (Discussion, Line 589) that the high spike density on SFV virions may compensate for partial loss of fusogenic activity following NMT inhibition. In contrast, SARS-CoV-2, RSV, and VSV have sparser surface spike densities, potentially making them more susceptible to spike impairments, leading to loss of infectivity.

4. Fig 2: overall, the results on ChPCOs organoids are currently preliminary and, in part, in contrast to the existing literature. In this model the authors showed SARS-CoV-2 infection of MAP2+ neuronal cells. However, it has previously been demonstrated that cortical neurons are not permissive to the infection and only <0.1% of neurons are infected by SARS-CoV-2 (PMID: 32579880; PMID: 33010822). Therefore, a more pure choroid plexus (ChP) model (PMID: 33010822; PMID: 33113348), quantifying infection (N protein) on ChP TTR+ cells, would be more appropriate for the question that the authors wish to address.
We thank the reviewer for this comment. We would like to clarify that the aim of the organoid experiments was to assess the role of NMTs in SARS-CoV-2 infection and spread specifically in neurons.

The reviewer is correct that SARS-CoV-2 infectivity in 2D and 3D neuronal models lacking a choroid plexus component has been consistently low -around 0.1% (PMID: 37039676, 38172412, 38749422, 37495586). However, the 3D model we employed includes neurons, immature astrocytes, and choroid plexus cells (PMID: 38838150; Fig. A, S2, S3), and exhibits significantly higher neuronal infection rates, averaging ~5% and exceeding 10% in cortical-like layers (PMID: 38838150; Fig. 2F). Moreover, our recent work shows that SARS-CoV-2 spreads among neurons over 72 h in this model (Kettunen *et al*., bioRxiv preprint: https://doi.org/10.1101/2024.11.21.624622, in revision). Based on this, we selected 72 hpi as the experimental endpoint to evaluate the impact of IMP1088. Our data show that IMP1088 efficiently inhibits viral spread and reduces the overall apoptotic index in organoids (Fig. 2G).

These findings highlight both the relevance of using a more complex, brain-like 3D model to study neuronal infection and the potential of IMP1088 as a candidate antiviral targeting neuronal spread. To assess NMT inhibition in a physiologically relevant epithelial context, we also included data from 3D nasal epithelial cells cultured at the air–liquid interface (Fig. 1T–W). We have incorporated the references suggested by the reviewer and now discuss differences between organoid models in the revised manuscript (Line 224).

5. Fig 2: the data shown, as far as one can conclude from the legend, are based on a single biological replicate and just two technical replicates. This is insufficient for stem cell based-disease modelling. The current ISSCR guidelines recommend the use of three hPSC/iPSC lines for stem cell studies. Furthermore, independent differentiation experiments (at least three biological replicates) are required to support the claims.

We apologize for the imprecision in the original figure legend. For initial characterization of the ChPCO model, we performed scRNA-seq using three pooled organoids from three replicates, all derived from a single cell line. This has now been clarified in the revised figure legend. Sequencing was conducted twice on independently pooled samples, and the results shown in Fig. 2A, S2, and S3 were consistent across replicates. The primary aim of the scRNA-seq experiment was to characterize the 3D choroid plexus–containing organoid model used in subsequent infection assays. We believe that the current dataset from pooled organoids provides sufficient characterization for this purpose.

For the drug treatment experiments, we have now included additional data from organoids derived from three independent cell lines, each with 3–4 biological replicates (revised Fig. 2C–G), in accordance with current ISSCR guidelines. These new experiments confirm our previous findings: treatment with IMP1088, Apilimod, or Nafamostat at 72 hpi significantly reduces both total and neuronal SARS-CoV-2 infection rates in the ChPCO model and lowers the apoptotic index.

Additionally, we repeated the re-infectivity assays using organoids from three different cell lines, each with 3–4 biological replicates. These updated results (Fig. S4H–K) demonstrate that SARS-CoV-2 released from IMP1088–treated A549-AT cells has markedly reduced infectivity, further supporting the potential of IMP1088 to block viral spread in the ChPCO model.

6. Fig 2: Moreover, it is unclear how the authors segmented the MAP2+ staining. It is not clear that MAP2 staining can accurately be segmented into individual neurons (if successful, such a segmentation strategy should be shown in the supplementary figures). If this is the goal (and one could argue that indeed one should not be interested in neurons but rather ChP cells), one could better segment individual nuclei using a marker such as HuC/HuD.
We would like to reiterate that the primary aim of the ChPCO experiments was to assess the potency of IMP1088 in inhibiting SARS-CoV-2 infection in neurons, rather than in choroid plexus cells. As suggested by the reviewer, we have now added a description of the MAP2-based segmentation strategy to the Methods section (Line 391).

Cell identification was based on 3D detection of DAPI-stained nuclei, while neuronal identity was determined by measuring MAP2 signal intensity in the perinuclear region. SARS-CoV-2 infection was quantified as the proportion of nucleocapsid-positive objects colocalized with segmented nuclei, normalized to the total number of nuclei. Neuronal infection density was assessed by calculating the area of nucleocapsid and MAP2 colocalization, normalized to the total MAP2-positive area. We have previously validated this approach in our recent study using the same 3D ChPCO model (PMID: 38838150), where both MAP2 and the pan-neuronal marker NEUN were used independently and yielded consistent results. MAP2 was selected here due to its strong signal intensity and ability to visualize neurite extensions, providing further confirmation of neuronal differentiation.

7. Fig 2: the authors provided the quantification of cleaved Caspase-3. Please show representative ICC images for these staining.
In response to comment 5 above, we have repeated the cleaved caspase-3 experiments using organoids derived from three independent cell lines, each with 3–4 biological replicates (Fig. 2G). Representative immunofluorescence images are now included in Fig. 2D.

8. In summary, the data in Fig 2 and in Supplementary figures 2, 3 and 4 do not add further value to the manuscript, and as such the authors should consider removing these data.

As noted above, SARS-CoV-2 infectivity is very low in 2D and 3D neuronal models that lack a choroid plexus component (PMID: 37039676, 38172412, 38749422, 37495586). In contrast, our 3D ChPCO model supports robust neuronal infection (PMID: 38838150; Fig. 2F). We have also shown that SARS-CoV-2 spreads among neurons over 72 hours in this model (Kettunen et al., bioRxiv preprint doi: https://doi.org/10.1101/2024.11.21.624622, in revision). In the current study, we demonstrate that IMP1088 treatment effectively inhibits this neuronal spread and reduces the overall apoptotic index in the organoids (Fig. 2F, 2G). These findings underscore the importance of using a complex 3D brain-like tissue model to study SARS-CoV-2 spread and antiviral efficacy. Models lacking a choroid plexus component -whether 2D or 3D- may not fully capture key aspects of brain infection. We therefore thank the reviewer for the comment but respectfully disagree with their point of view.

9. 'We observed significantly decreased levels of infection caused by virions released from IMP-1088-treated cells compared to those released from DMSO-treated cells (Figs. 2I-J)'. At which time points were the supernatants from infected cells collected? Has the amount of SARS-CoV-2 been added to the organoids at equal amount? Please provide more experimental details.
Released virions were quantified by qRT-PCR, and an equal viral input (1×10^6 SARS-CoV-2 Wuh genome copies) was used for re-infection across all experiments. To clarify the complex experimental design, we have now included a schematic in Fig. S4H and updated the corresponding figure legend and Methods section accordingly.

10. Fig 3 A-B: the qRT-PCR results showed at the different time point from 0 up to 48h hpi should be included in a single plot using the same axes.
We have modified the figure as requested (please see updated Fig. 4J).

11. 'In contrast, analysis of the S protein, which is key to the viral infectivity, indicated that virions released from IMP-1088-treated cells contained significantly less total S protein..'. In Fig 3F, it is not clear whether the western blot has been performed from cell lysate or supernatants. The authors claim that the virion released has less S cleaved protein. To this aim, the virus should be collected from the supernatants and purified by ultracentrifugation and the western blot should be performed on the purified viral particles.
We agree with the reviewer that the original text lacked clarity. We have now clarified in the Methods section, main text, and figure legends that the western blot was performed on virions released into the extracellular medium and purified by sequential ultracentrifugation. Viral load was quantified by qRT-PCR, and equal amounts of viral RNA (based on copy number) were loaded per lane on the SDS-PAGE (Fig. 3P). Additionally, we have replaced the original western blot with a shorter exposure to better resolve the S1 and S2 fragments.

12. For Fig 4, while providing interesting leads on how NMT inhibition in the host may affect virion infectiousness, the data would be better combined with the experimental data in Fig 5 which validate the key pathways that are perturbed by IMP-1088 treatment.
The two figures have now been combined as requested (please see modified Fig. 5).

13. Fig 5: Considering how IMP-1088 affects A549-AT cells and the magnitude of the phenotypes seen in the ERGIC and Golgi apparatus, the authors should validate these findings in the disease-relevant models used in Fig 1 (e.g. nasal epithelium and human lung) for both the ERGIC-53 staining, the GM130 staining, and importantly test for cytotoxicity in all models used (this also considering the changes in Actin staining seen in Fig 6).

Our A549-AT cell line is a human lung cell model, and the effects of IMP1088 on these cells are thoroughly characterized in Fig. 5. Cytotoxicity of IMP1088, as well as the combined effects of drug treatment and SARS-CoV-2 Wuh infection on cell viability, are now comprehensively addressed in Fig. S1D and S1E. No significant reduction in viability was observed at IMP1088 concentrations up to 1 µM compared to DMSO controls (Fig. S1D). At 10 µM, IMP1088 caused a modest (~20%) but significant decrease in viability, substantially less than the strong cytotoxic effects of puromycin and UNC-01 (Fig. S1D). To assess the combined effects of drug treatment and viral infection, A549-AT cells were treated for 48 h with DMSO or IMP1088 (3.9 nM–10 µM). SARS-CoV-2 Wuh infection alone caused ~20% reduction in viability (Fig. S1E), but IMP1088 treatment did not further reduce viability at any tested concentration.

We also evaluated IMP1088 in human nasal epithelial cells from three adult donors cultured under submerged conditions and treated for 48 h with DMSO, IMP1088, or puromycin (Fig. S1F). At 1 µM, IMP1088 had no effect on viability in two donors and caused a slight decrease in one. In contrast, 10 µM IMP1088 and 2.5 µM puromycin significantly reduced viability or showed a downward trend in all donor samples.

Additionally, we tested IMP1320, a water-soluble analog of IMP1088, for cytotoxicity and antiviral activity. A 48-h treatment with IMP1320 in SARS-CoV-2–infected A549-AT cells showed antiviral efficacy comparable to IMP1088, without significant cytotoxicity at concentrations between 7.8 nM and 1 µM (Fig. S4A-C). IMP1320 has been evaluated in vivo and shown to be effective and well-tolerated in eliminating MYC-deregulated tumors (Lueg et al., 2021, bioRxiv doi: https://doi.org/10.1101/2021.03.20.436222, in revision). Additional in vivo data from Pacylex (PMID: 35323358) further support the safety profile of NMT inhibitors, which are now being tested in cancer patients in clinical trials.

Together, these findings demonstrate that NMT inhibition is well-tolerated *in vitro* and *in vivo*, presenting a valuable candidate for future antiviral therapies, possibly in combination with other active compounds. Based on these extensive cytotoxicity and efficacy data, and the published in vivo and clinical trial results mentioned above, we did not further assess IMP1088 toxicity in ChPCOs, or characterize its effects on ERGIC and Golgi in nasal epithelium, as the antiviral efficacy and tolerability had already been established in relevant lung and nasal epithelial models.

14. ‘Unexpectedly, in IMP-1088 treated cells, we also observed the release of virions from structures resembling ER (Fig. 7D). In support, electron tomography (ET) analysis revealed small opening from ER to the plasma membrane (Fig. 7E).’ In Fig 7D seems that the treatment of IMP-1088 increases the number of vesicles. Have the authors quantified whether the number of vesicles is higher in treated cells compared to DMSO? Can the authors further investigate if the virus is trapped within these vesicles?

We apologize if our original description was unclear. In the EM images, the small electron-dense particles are not vesicles, but SARS-CoV-2 virions (indicated by arrowheads) located within the lumen of an abnormally dilated ER compartment, which forms in response to IMP1088-treatment (Fig. 7J). A clear opening from this ER compartment to the extracellular space is visible in the 3D tomogram (Fig. 7K, inset “ii”; arrow). In inset “i” of the same figure, these virions are pseudo-coloured in brown. In other words, the small round structures observed in the EM images represent SARS-CoV-2 virions, not vesicles.

Minor critiques:

1. Fig 1D: the authors showed that the inhibition of N-myristoyltransferases reduces the formation of syncytia formation. Please provide quantification of these data.
The quantification of syncytia is now shown in Fig. 1G.

2. Fig 3C: the images do not represent the graph, although the quantification show a reduction of N protein compared to the DMSO treated cells, the staining of N protein in Wash- condition in IMP-1088 treated cells is higher compared to the non-wash condition. Please provide representative and high-quality images (perhaps these were lost with PDF compression).
We thank the reviewer for noticing the error. The panel had been swapped by mistake. We have now updated the image panel, and 'wash' and 'no wash' representative images are now shown correctly in Fig. 4L.

3. There is an error in the correspondence of the letters between the text and the figures: (Fig 5F, G) is the 5H, 5I. (Fig 5H) is 5L. (Fig 5H) is 5L. Fig 5J is 5N.
We apologise for these errors and have now corrected the mistakes.

4. There are some minor typo's throughout the manuscript. Please address these and if possible add line numbers to easily identify such errors.
We have now added the line numbers to the manuscript and corrected typos.

Reviewer #2 (Remarks to the Author):
I co-reviewed this manuscript with one of the reviewers who provided the listed reports. This is part of the Nature Communications initiative to facilitate training in peer review and to provide appropriate recognition for Early Career Researchers who co-review manuscripts.
We thank you for your contribution.

Reviewer #3 (Remarks to the Author):
This manuscript reports an interesting observation that NMTs inhibitor IMP-1088 displayed very robust inhibition effects on the assembly and/or release of SARS-CoV-2 in cell lines, in primary human nasal epithelial cells, and in brain organoids, which was due to disruption of conventional secretory pathway and activation of Golgi-bypassing lysosomal exocytosis. IMP-1088 also inhibits RSV infection, probably by a similar mechanism. Overall, the conclusions will be interesting to the field and a number of experiments and volume of data are presented. However, the conclusion is not strongly supported. Most experiments are based on the inhibitor IMP-1088 treatment and manipulation of NMTs protein is missing. Also, validation of the identify of key protein or proteins downstream of the NMTs, whose N-myristoylation is required for SARS-CoV-2 assembly, is lacking. For some results, additional detail and explanation would be helpful. The following concerns need to be addressed before considering acceptance for publishing in Nature Communications.

Specific major comments:

1. Previous study showed that N-myristoyltransferase 1 is essential for mice embryo development but is not essential for cell lines, and NMT-1 knockout cells displayed 95% reduction of the NMT activity. NMT-1 knockout or knockdown (if not NMT1/NMT2 together) should be performed to test its effect on SARS-CoV-2 assembly and secretion.

We thank the reviewer for this valuable comment. In response, we generated stable A549-AT cell lines with CRISPR interference-mediated knockdown of either NMT1 or NMT2 to evaluate their respective roles in SARS-CoV-2 infection (Fig. 3).

Western blot analysis confirmed partial knockdown of NMT1 using a single sgRNA (Fig. 3A), which resulted in a significant reduction in SARS-CoV-2 Wuh infection at 48 hpi compared to cells transduced with a non-targeting sgRNA control (Fig. 3B, C). To ensure that the non-targeting sgRNA had no off-target effects, we compared infection rates in parental A549-AT cells and cells expressing the non-targeting sgRNA. Both showed comparable infection rates (Fig. 3D), and IMP1088 treatment (0.0039–1 µM) inhibited SARS-CoV-2-mCherry infection to similar levels in both lines, confirming that the control sgRNA did not alter viral susceptibility (Fig. 3D). To achieve a stronger NMT1 knockdown, we combined sgRNAs 1–3, resulting in near-complete loss of NMT1 protein (Fig. 3E). This enhanced knockdown led to an approximately 60% reduction in SARS-CoV-2-mCherry infection at 48 hpi compared to controls (Fig. 3F–H). Importantly, IMP1088 still inhibited infection to similar levels in both control and NMT1 KD cells (Fig. 3H), suggesting that residual NMT1-independent activity remains drug-sensitive. In contrast, stable NMT2 knockdown using sgRNAs 1–3 resulted in undetectable NMT2 protein (Fig. 3I) but had no effect on SARS-CoV-2-mCherry infection (Fig. 3J–L). Together, these results indicate that NMT1 is the primary mediator of the antiviral effect, while NMT2 may provide partial compensation in its absence.

2. IMP-1088 treatment did not display inhibitory effects on the viral RNA release at 12 hpi. At 12 hpi, does IMP-1088 treatment reduce the viral infectivity of release viruses? Also, at 12 hpi, does IMP-1088 treatment reduce viral protein (S, M) levels in media by WB? This is an important question since multiple rounds of infection will make the results very difficult to interpret. One replication cycle for SARS-CoV from absorption to release of infectious virions is about 7-8 hours, which is probably the similar case for SARS-CoV-2. To test the viral infectivity of release virions, released viral RNA amount, and released viral protein levels, with and without IMP-1088 treatment, in one but shorter than two SARS-CoV-2 replication cycles, is highly recommended to strengthen the manuscript's conclusion.
As suggested by the reviewer we assessed the infectivity of the virus in new experiments at 12 hpi, 24 hpi and 48 hpi. In short, A549-AT cells were treated with DMSO, 1 µM IMP1088 or a combination of 0.25 µM Apilimod and 20 µM Nafamostat, at 1.5 hbi, and then infected with SARS-CoV-2 Wuh for 12, 24 or 48 h. After this, released virions were collected from the culture media, and then used to infect VEROE6/ TMPRSS2 cells (based on qRT-PCR: 1x10^4 copy number for 12 hpi time point, 1x10^5 for 24 hpi, and 1x10^6 for 48 hpi) for 8 h (Fig. S4F). The percentage of infected VEROE6/ TMPRSS2 cell were then quantified based on N-positive cells normalized number of nuclei (Fig. S4G). The results show that the infectivity of the virions released from IMP1088-treated cells is compromised already at 12 hpi (Fig. S4G).

WB could not be performed at this early time point (12 hpi), due to insufficient amount of released virions (as a comparison, please see Fig. 4O showing the WB of cell lysate, which shows only faint bands for S and N at 12 hpi).

3. In Figures 3F and 3H, what about the S and M protein blots in the cell lysates? It will be more convincing if these assays could be done for a short infection time (from 1 to shorter than 2 cycles).
We have now performed new experiment to address this. A549-AT cells were treated with DMSO or 1µM IMP1088 at 1.5 hbi and infected with SARS-CoV-2 Wuh for 0-48 h. Cell lysates were collected at 0, 6, 8, 12, 24 and 48 hpi and analysed by WB (Fig. 4P). The effect of

the drug is only seen post 12 hpi. As we saw no differences in the levels of S protein in the cell lysate at early time points (Fig. 4O), we did not test the M at this time point.

4. An intracellular viral titer assay (measuring the viral infectivity of virions inside the cells) is required to confirm that IMP-1088 treatment indeed disrupts SARS-CoV-2 assembly and produces less infectious virions. It will be good to perform it for a short time of infection (shorter than 2 replication cycles).
While this would be interesting, SARS-CoV-2 particles assemble and bud into the lumen of the secretory pathway, i.e. ER/ ERGIC. Isolation of intracellular virions would require harsh homogenization or the use of detergents, both of which are harmful to the structure and infectivity of the virions. To our knowledge, isolation of SARS-CoV-2 intracellular and intact virions is, thus, not feasible. However, in support of our interpretation of decreased infectivity of released virions, our electron microscopy studies indicated that while progeny particles are formed efficiently (Fig. 6B), the virions released from IMP1088-treated cells demonstrated decreased levels of spike, and M protein (consistent with lower amount of glycosylated M) compared to viruses isolated from vehicle-treated control cell media (Fig. 4P-S). These results show that upon inhibition of NMTs, the structure of the released virions is altered.

5. For the cellular viability assay, A549-AT cells treated with IMP-1088 and infected by SARS-CoV-2 should be tested. It is possible that IMP-1088 treatment alone does not cause cell death, but the combination of IMP-1088 treatment and SARS-CoV-2 infection induces a significantly higher cell death rate than SARS-CoV-2 infection alone.
As suggested by the reviewer, we have now performed cell viability assays comparing drug-treated cell to drug-treated infected cells. The results show that the drug-treatment did not decrease viability of infected cells (Fig. S1E).

6. It is an interesting observation that among 4 viruses that do not have N-myristoylation viral proteins, NMTs inhibitor selectively inhibits SARS-CoV-2 and RSV, but not SFV and VSV, although all these 4 viruses are enveloped single-stranded RNA viruses. SFV, VSV, and RSV are assembled at the host cell plasma membrane, but NMTs inhibitor only inhibits RSV but not the other two. More comments on this will be good.
We appreciate the reviewer's comment. We have addressed this in the response to Reviewer 1, comment 3, above by performing new experiments. In short, using a lower MOI 0.001 for SFV and VSV for 24 h infection, and by pre-treating A549 cells with 0.1-1 μM IMP1088 at 1 hbi or 24 hbi, we found that only SFV is not affected by the treatment (Fig. 1O-S). A discussion on why this virus is not as sensitive to the treatment as the other selected viruses is now included in the Discussion (Line 612).

7. The authors hypothesized that IMP-1088 treatment disrupted the secretory pathway and activated an alternative SARS-CoV-2 egress pathway which bypassed the Golgi apparatus, but lysosomal exocytosis of SARS-CoV-2 without any NMTs inhibitor treatment was proposed in reference 11, 12, 52, etc. Are the authors arguing that under normal conditions, SARS-CoV-2 exits the host cells via the conventional secretion pathway?
We do not argue that under normal conditions, SARS-CoV-2 exits the host cells via the conventional secretion pathway. Based on the current understanding of Coronavirus assembly and egress, the virions are believed to reach the Golgi compartment where the viral E, M, spike must be glycosylated and, in the case of SARS-CoV-2, the spike is cleaved by furin. From the Golgi compartment a transport mechanism to the lysosomes has been proposed, which in turn results in delivery of mature virions to secretory lysosomal vesicles that have a neutral pH. In this paper, we present evidence that upon NMT inhibition, the virions accumulate in a vesico-

tubular pre-Golgi compartment (that is positive for ER-marker calreticulin) where the furin cleavage is less accessible. From this compartment virions are either directedly released to the extracellular space or diverted to lysosomes and then released from there.

In support of this aberrant secretion mechanism, we demonstrate that ectopically expressed SARS-CoV-2 spike (S^{wt}) which, in the absence of other viral components, is retained in the secretory pathway (mainly ER and Golgi) and not secreted outside of the cells, is increasingly trafficked to the extracellular side of the cells following IMP1088-treatment (Fig. 7C). In further support of this egress mechanism, we now provide quantitative analysis of SARS-CoV-2 spike colocalization with endogenous lysosomal marker (LAMP1) inside the cell and at the cell surface at 48 hpi. The results show that in IMP1088-treated cells the spike colocalization with LAMP1 increases significantly inside the cell and at the cell surface (Fig. 7D-F). Furthermore, endogenous lysosomal protein LAMP1 and intralumenal ER protein calreticulin show increased colocalization with the ectopic S^{wt} secreted outside A549-AT cells (Fig. 7I and 7N, respectively), indicating a secretion event of these virus-containing compartments.

Specific minor comments:

1. It is very surprisingly impressive that 1-minute IMP-1088 treatment is as robust as 48-hour treatment in inhibiting the infection rate. It will be interesting and strengthen the authors' conclusion to test the effects of 1-minute IMP-1088 treatment on SARS-CoV-2 assembly, secretion, ER and Golgi structure. N-myristoylation is an irreversible modification. One-minute treatment may efficiently block the myristoylation of nascent proteins but not existing proteins. How can one-minute treatment displays such a robust inhibition of viral infection needs more explanation and discussion.
The reported constant of dissociation for IMP1088 is in the picomolar range (Kd < 210 pM; Mousnier *et al.* 2018 Nat Chem). Thus, in cell culture models, once IMP1088 binds the hydrophobic pocket of the NMT enzymes, the compound acts as a close-to-irreversible molecule. Mousnier *et al.* 2018 showed that when cells were pretreated with concentrations as low as 50 nM, reversibility of NMT inhibition occurred only 24 h after drug wash, which is very impressive, indeed, and confirms the demonstrated slow turnover of human NMTs (Thinon *et al*. 2014, Nat Com). We have now added these considerations in the main text (Line 189).

2. For the virus entry assay (Figure 1H-J), a more detailed description (for example, MOI, and whether viruses are washout) or method is needed. Also, 8 h infection is a little bit long. The virus entry assay in this study (PMCID: PMC10130743) is well-performed and more convincing.
As requested by the Reviewer, we have repeated the entry assays at 6 hpi, showing that IMP1088 does not affect the viral entry even when the drug was added 24 hbi (Fig. 4A, 4E). We have clarified the experimental design by adding a schematic outline of the experiment (Fig. 4A) and included a more thorough description in the figure legend and Methods.

3. For EM imaging, 48 h infection is a little bit too long. The shorter the time of infection, the better for observing the subcellular ultrastructure dynamics. For example, in Figure 6B, viral particles were notably absent in the ERGIC and Golgi apparatus of IMP-1088 treated cells, which was likely due to the lower infection in IMP-1088 treated cells at 48 hpi.
The cells shown in Fig. 6B are highly infected as evidence by a large number of virions in the enlarged ER lumen, clustered membranes (CMs), and large vesicle containing vesicles (LVCVs). In IMP1088-trated cells at 48 h, virions appear not to reach ERGIC and Golgi

membranes (Fig. 6B). In addition, virions also accumulate in lysosomes (Fig. 7B). As suggested by the reviewer, in addition to the 48 hpi panels we now provide addition panels obtained at 24 hpi (Fig. S7). The results obtained in the two time points are similar, in drug treated cells the virus accumulates in the lumen of a dilated ER compartment. Some virions are observed in dilated ERGIC, while Golgi apparatus, which mostly seen as dilated membrane stacks without a clear polarisation, is mainly observed void of virions. Earlier time points were not performed because the antiviral effect on the released virions was observed only after 24 h (see kinetics of virus release and infectivity of progeny virions in Fig. 4G-J). We would like to also point out that for the EM analysis we selected only highly infected cells where virions were readily identifiable.

4. It was reported that SARS-CoV-2 mediated Golgi fragmentation accelerated viral assembly and trafficking. Can authors make some comments on it?
These two phenomena are separate. The virus-induced Golgi fragmentation, which accelerates virus trafficking and release does not prevent the virions to access Furin-containing Golgi compartment (PMID: 35291301). The alteration of the secretory compartment induced by IMP1088, which does not favour virus assembly, release, and infectivity, prevents the trafficking of viral components from early to the late secretory pathway, thereby impairing the maturation of S and M and their incorporation to the new progeny virions.

5. Both references 72 and 73 referred to VSV assembly, and the SFV assembly citation was missing.
Apologies for the mistake, which has now been corrected.

6. On page 9, Hela should be HeLa, reference 19 was put inside the word.
The typo and the unnecessary reference have been corrected.

7. On page 7, We was written as Wwe.
This has been corrected.

Reviewer #4 (Remarks to the Author):
Overall, this is a well designed and reported study with some significant potential impact on human health as it relates to some viral infections. The rationale is sound, results support the major conclusions and the manuscript is written well. While using the organoid-derived approach to increase human disease relevance and human donor nasal cells were included, the relevance of these "artificial" growth lacking full human microenvironment is still a concern, although one that may be limited to overcome.

1) Validation of the findings in animal models is lacking and would be the next step to more fully characterize the mechanisms in a fully competent microenvironment model, specifically to understand the impact of NMT inhibition on normal homeostasis. Specifically, how will non-infected cells or other cells systemically be impacted by inhibition of NMTs.
We agree with the reviewer and to this end we have now assessed the antiviral potential of a water-soluble derivative of IMP1088, called IMP1320, in cultures. These results demonstrate that IMP1320 has similar antiviral efficacy than IMP1088 in A549-AT cells infected with SARS-CoV-2 Wuh (Fig. S4A-C). This drug has been tested *in vivo* to eliminated MYC-deregulated tumors, showing efficacy and tolerability data that demonstrates that the drug has no overt toxicity (Lueg et al., 2021 N-myristoyltransferase inhibition is synthetic lethal in

MYC-deregulated cancers, bioRxiv preprint doi: https://doi.org/10.1101/2021.03.20.436222, in revision). Pacylex have also published *in vivo* data with their NMT inhibitor (PMID: 35323358), and it is now being dosed in cancer patients in clinical trials. Together, these findings demonstrate that the NMT inhibition, while being well-tolerated *in vivo* and currently in clinical trials for cancer research, also represent a valuable candidate for future antiviral therapies, possibly in combination with other active compounds. We have included these considerations to the Discussion (Line 658).

2) Also, using genetic perturbations (CRISPR/RNAi) to validated the drug activity vs off-target effects driving the phenotype would be important.
This has been addressed above in response to Reviewer 3 comment number 1 (Fig. 3). In short, we created stable A549-AT cells with knockdown of NMT1 or NMT2. SARS-CoV-2 infection in these cell lines was decreased proportionally to the level of NMT1, but not NMT2, indicating that in these cells NMT1 is the main driver of the antiviral activity of IMP-1088.

Overall, this is a well rounded study with very interesting conclusions. Minor comments: figure 4 resolution is lower than ideal.
We have now provided a higher resolution image.

Reviewer #5 (Remarks to the Author):
The manuscript titled "Inhibition of host N-myristoylation compromises the infectivity of SARS-CoV-2 due to Golgi-bypassing egress from lysosomes and endoplasmic reticulum" by Saber et al. presents data on the antiviral activity of IMP-1088, an inhibitor of cellular N-myristoyltransferases (NMT), and investigates the mechanisms of action in an infection by a virus without known myristoylation sites, which is a relevant extension to previously published work on NMT inhibitors in viral infections (Mousnier et al., Nat Chem. 2018).
The research offers interesting insights into a potential new therapeutic option for specific viral infections, including Sars-CoV-2 and RSV. Overall, the manuscript is well-written, and the presentation of the results is largely comprehensive. Nevertheless, there are certain shortcomings that should be addressed. I have provided my comments and suggestions below.
I hope my comments will be helpful in revising the manuscript. I am confident that with these revisions, the paper will make a valuable contribution to the field, and I recommend accepting the manuscript with major revisions addressing the comments below.

Major Comments:

1. The authors present an extensive dataset investigating the therapeutic potential of NMT inhibition. However, the study focuses solely on in vitro experiments and cellular models and lacks a discussion on the pharmaceutical usability of NMT inhibitors and potential adverse side effects. Although in vivo testing of NMT inhibitors may not be within the scope of this study, the manuscript would benefit from a discussion of the limitations of the cell lines, in vitro models, and organoid systems employed. This would provide valuable context to the reader and help to evaluate the translational potential of the findings.
We have addressed this question above in Reviewer 4 comment 1. In short, to this end we have now assessed the antiviral potential of a water-soluble derivative of IMP1088, called IMP1320, in cultures. These results demonstrate that IMP1320 has similar antiviral efficacy than IMP1088 in A549-AT cells infected with SARS-CoV-2 Wuh (Fig. S4A, S4B) without inducing cytotoxicity (Fig. S4C). This drug has been tested *in vivo* to eliminated MYC-deregulated tumors, showing efficacy and tolerability data that demonstrates that the drug has no overt

toxicity (Lueg et al., 2021 N-myristoyltransferase inhibition is synthetic lethal in MYC-deregulated cancers, bioRxiv preprint doi: https://doi.org/10.1101/2021.03.20.436222, in revision). Pacylex have also published *in vivo* data with their NMT inhibitor (PMID: 35323358), and it is now being dosed in cancer patients in clinical trials. Together, these findings demonstrate that the NMT inhibition, while being well-tolerated *in vivo* and currently in clinical trials for cancer research, also represent a valuable candidate for future antiviral therapies, possibly in combination with other active compounds. We have included these considerations to the Discussion (Line 658)

2. Page 3 "Our findings demonstrate that inhibiting NMT1 and NMT2 in human lung and primary nasal epithelial cells, as well as in human 3D choroid plexus-cortical neuron organoids, disrupts viral assembly and maturation by interfering with the host cell's secretory pathway membrane trafficking." The authors state here that they show effects in "human lung […cells]". The model they use are "human lung small carcinoma cells that were engineered to stably express the virus receptor ACE2 and protease TMPRSS2, […]". Please indicate that the experiments were done using a cancer cell line and not primary human lung specimen.
We have now clarified this in the text.

3. Figure 2 A/B, as well as Suppl Figure 2 and 3, show the scRNA-seq data of the ChPCOs as UMAP representations and the expression of key genes as feature plots. These plots are hard to read and give little quantitative information about the gene expression per cluster. As shown in Suppl. Fig 4, visualization of the gene expression per cell type as violin plots or a dot plot allows to understand the number of cells expressing the gene and the relative average expression level of the gene much better. Specifically, ACE2 and TMPRRS2 seem to be detected only in very few cells. Using a dotplot, the expression of all genes shown in Figure 2 and Suppl. Figures 2, 3 and 4, could be easily summarized in a single figure giving a much simpler, yet more comprehensive and informative visualization of genes expression in the main figure 2.
We thank the reviewer for the suggestion and have now replaced the Fig. 2, Fig. S2 and Fig. S3 UMAPs with violin plots that are now collated to new Fig. S2 and Fig. S3. With these changes, the original Fig. S4 became and was therefore removed.

4. Page 7: "In addition, Wwe also quantified the level of SARS-CoV-2 infection in ChPCOs using virions released from either DMSO or IMP-1088-treated cells (Fig. 2E)." Please specify in which cells these virions were produced.
Virions were collected from A549-AT cells, which has now been indicated in the revised Results section of the main text, Methods, along with the Figure legend (Fig. S4H-K).

5. In the single cell RNA-seq data of ChPCOs, what is the expression level of NMT1 and NMT2? Which cells, if any, show a high expression?
We have now included bar blots of NMT1 and NMT2 expression in Fig. S3B. Based on the scRNAseq, NMT1 is expressed widely in different cell types, NMT2 is mainly expressed in inhibitory neurons and proliferating neural stem cells (NSC).

6. According to the "Data and Code Availability" section, the authors do not intend to publish the code used for the transcriptomics analysis. I strongly recommend publication of the code for the community to have a chance to reproduce and evaluate the analyses performed in this study. This is currently not possible and hampers the evaluation of the manuscript.
We apologise for the if our text was not clear. We intent to publish the code. We have denoted the code for annotating CP organoids to GitHub with link

https://github.com/huiwenzh/CP_organoids. The GEO accession number and token has been sent to the Editor, who will circulate this to reviewers requiring access to the private data. Once accepted for publication, the GEO accession number and token will be made public.

7. Please clarify if the ChPCOs used in this study were derived from multiple donors or all from a single donor?
As an initial characterization of the organoid model, we used scRNAseq of 3 pooled organoids from 3 repetitions originating from a single donor cell line. The sequencing of these pooled samples was performed twice and the results shown in Fig. 2A, S2 and S3 were consistent. On the other hand, in our infection tests, we have now included results from organoids originating from 3 different donor cell lines and each with 3-4 biological replicates (updated Fig. 2B-G, S4H-K), which is compliant with the current ISSCR guidelines. These details are now included in the respective Figure legends and Methods section.

8. The presentation of the single-cell RNA-seq data does not allow to evaluate the cell type annotation. Please include a dot plot of all marker genes determined using the FindAllMarkers function and used for cell type annotation in the supplementary figures as described in the methods section under "scRNA-seq analysis".
As requested by the reviewer, we have now applied FindAllMarkers function across clusters to identify DEGs (markers), and then selected known cell type markers based on literature or expert input. We have included the top 50 markers identified per cluster using FindAllMarkers in the Table 3.

9. The access token provided for the review of the GEO submission is not working. Please check if the token is correct and still valid.
We apologise for the data not being available for the reviewer. The GEO accession number and token has been sent to the Editor, who will circulate this to reviewers requiring access to the private data. Once accepted for publication, the GEO accession number and token will be made public.

10. Page 8: "Following our findings of host cell NMT inhibition leading to a significant decrease in infectivity of the released virions and the perturbed trafficking of the viral particles to ERGIC and Golgi compartments, we next explored the potential impact of this transport blockage on the structural proteins of the released virions." The perturbed trafficking of the viral particles to ERGIC and Golgi has not been shown at this point in the manuscript.
We apologize for the mistake and have now modified the order of results.

11. Page 8 "We observed slightly decreased levels of the viral N protein, which is important for viral genome packaging, in virions released from both DMSO and IMP-1088-treated cells (Figs. 3F, 3G)." Slightly decreased in comparison to what?
The comparison was made to DMSO vehicle control. We have now modified the main text to clarify this point and in the respective Figure legend (Fig. 4Q).

12. Page 9: "The inhibition of cellular NMT led to significant changes in the abundance of proteins across multiple subcellular pathways (Fig. 4A), particularly those involved in the early secretory pathway endoplasmic reticulum (ER), ER-Golgi intermediate compartment (ERGIC), and Golgi apparatus and vesicle trafficking (Figs. 4B)." Please discuss potential adverse side effects of this fundamental effect on the proteome?
We thank the reviewer for this comment. We have now included the requested considerations in the Discussion.

13. Page 9, “NMTs regulate protein homeostasis”. Please specify in the main text how the Gene Set enrichment analysis was performed and which annotation data base was used.
As requested, the following text has been added to Line 411 of the main text: “Gene Set Enrichment Analysis (GSEA) was performed using clusterProfiler[42] on the entire ranked protein list based on ranking by log fold-change (IMP-1088 treatment versus DMSO control). Proteins that mapped to gene symbols associated with the ‘biological processes’ ontology were derived from the R/Bioconducter annotation of human gene symbol as provided for in ‘org.Hs.eg.db’. The minimum gene set size was set to 5 and a p-value cutoff of 0.05 (after adjusting for multiple hypotheses using the Benjamini and Hochberg method) were retained.”.

We also added more details of this to Line 580 in the Methods: “Gene Set Enrichment Analysis (GSEA) was performed using clusterProfiler[42] (version 4.10.0) on the entire ranked protein list, ranked by log fold-change (IMP treatment versus Control). Proteins that mapped to gene symbols associated with the ‘biological processes’ ontology were derived from the R/Bioconducter annotation of human gene symbol as provided for in ‘org.Hs.eg.db’ (database version 3.18.0). The minimum gene set size was set to 5 and a p-value cutoff of 0.05 (after adjusting for multiple hypotheses using the Benjamini and Hochberg method) were retained. Analyses were performed in R version 4.3.2.”.

14. Page 9, “Further analysis revealed a significant decrease in the abundance of proteins with N-terminal glycine destined for N-myristoylation (Fig. 4C).” Please extend the description of this figure and explain the analyses and comparisons done here to published data.
As requested, the following description has now been added to Line 422: “Following reanalysis of Mousnier *et al.* 2018, NMT predicted targets (based on N-terminal motif presence in the current experiment), were classified by experimental validation as previously described[59]: false negative (predicted only), true positive (predicted and experimentally detected) and if verified as a YnMyr positive target (grey outlines[59]). NMT targets (red) were enriched as decreasing with IMP treatment (odds ratio of 10.36982, p-value 6.009e-05), also confirming the effect in previously reported N-myristoylated proteins (grey outlines[59]) (Fig. 5C).”. We have also updated the key in Fig. 5C to clarify the description of the results more clearly.

15. Page 10 “A treatment with 5 µg/mL BFA for 40 s or 4 min led to a loss of the Golgi localization and to a homogenous distribution throughout the cell (Fig. S6A,B). These effects were different from IMP-1088, where we discovered that the treatment with 1 µM IMP-1088 for 1h or 48 h induced a gradual dispersal and fragmentation of Arf1-GFP signal (Fig. S6C; Note the considerably longer treatment), supporting previous findings that NMT inhibition blocks coatomer complex I (COPI) assembly and results in Golgi dispersal51. We observed a gradual increase in the mean fluorescence intensity (Fig. S6D), along with decrease in the mean spot size (Fig. S6E), and an increase in the number of spots (Fig. S6F), of ARF1-GFP following IMP-1088 treatment. Together, these results indicate that the effects of IMP-1088 to the secretory pathway organelle morphology and trafficking are different from BFA, which is a well-established inhibitor of ARF1.” The authors specifically mention the considerably different treatment times. How are these findings comparable?
We apologise that this experiment was not clearly explained. We chose to compare the effects of NMT inhibition with IMP1088, which is known to block COPI assembly and results in Golgi dispersal (PMID: 38012402) to BFA, which is a widely used and well documented drug that inhibits Arf1 and perturbs ER-Golgi membrane trafficking. BFA targets ARF1 almost instantaneously (i.e. effects shown at 40 s and 4 min timepoints), while the effects of IMP-1088 on Arf1 is considerably slower. To highlight this, we have now included a time course of this

in new Fig. S6E showing that 1 µM IMP-1088 treatment does not noticeably affect ARF1-GFP at 40 s, 4 min, 20 min, 30 min, 40 min, or 50 min time points. Only modest effects appear at 1 h incubation, which then gradually become more profound in the course of 48 h-treatment (Fig. 6SF-I). These findings highlight the two different time frames required for these two drugs to produce their maximal effects.

This clarification has now been added in the manuscript Line 492: "In live A549-AT cells transiently expressing ARF1-GFP, ARF1 localized to the perinuclear region, consistent with Golgi association (Fig. S6A). Treatment with 5 µg/ml BFA caused rapid dispersal of ARF1-GFP within 4 minutes, resulting in a diffuse cytoplasmic signal with no changes in the overall fluorescence intensity, indicating redistribution rather than degradation (Fig. S6A-D). In contrast, 1 µM IMP1088 had no immediate effect on ARF1-GFP localization (40 s–4 min), and only modest alterations were observed after 1 h (Fig. S6E–F). Even after 48 h, ARF1-GFP remained membrane-associated, though with reduced spot size and increased puncta number, supporting our EM findings of changed secretory pathway organelle structures, while total ARF1-GFP intensity remaining unchanged (Fig. S6F-I). These results indicate while both BFA and IMP1088 perturb secretory pathway membrane trafficking, the effects occur at different time scales. BFA directly traps ARF1 in its GDP-bound state, blocking activation and membrane association of the protein. NMT inhibition, on the other hand, disrupts COPI function and induces Golgi dispersal29 significantly slower. In support of this, IMP1088 only results in inhibition of N-myristoylation of newly synthesized NMT substrates, and not of pre-existing N-myristoylated proteins.".

16. The manuscript has no information or discussion on the potential application of NMT inhibitors in humans and adverse side effects. Please include these topics in the discussion and elaborate on the pharmaceutical use of such drugs.
This question was also raised by Reviewer 4 (Comment 1). We agree with the reviewer that this is an important discussion topic, and to this end we have now assessed the antiviral potential of a water-soluble derivative of IMP1088, called IMP1320, in cultures. These results demonstrate that IMP1320 has similar antiviral efficacy than IMP1088 in A549-AT cells infected with SARS-CoV-2 Wuh (Fig. S4A-C). This topic is discussed in Line 658.

17. Line numbering would have been very helpful for the reviewing process. Please include line numbers in any future versions of this manuscript.
The line numbering has been added to the manuscript file.

Minor comments:
1. Fig. 1R: the x-axis ticks are off.
Thank you for noticing the mistake. We have addressed the Comment 3 made by Reviewer 1 above and replaced the figures 1P-R with new results and graphs (new Fig. 1O-S).

2. Fig. 2A: "umap_3" on y axis.
The axis has now been corrected to "umap_2".

3. Fig. 2C: I do not understand why the UMAP in Fig 2C is its own panel compared to the UMAPs shown in Fig. 2B.
In Fig. 2B, the markers were shown for SARS-CoV-2 related ChPCO proteins. Fig. 2C, on the on the hand, showed the distribution of the neuronal marker MAP2 in the cells analysed (which is relevant to SARS-CoV-2 neuronal infection in ChPCOs, Fig. 2F). To void confusion, we have now compiled choroid plexus (Fig. S2A), progenitor (Fig. S2B), and neuronal cells (Fig.

S2C), as well as SARS-CoV-2 infection related protein expression profile (Fig. S3A) and NMT1 and NMT2 (Fig. S3B) in their respective figures.

4. Page 7: "Compared to control organoids treated only with vehicle (DMSO), those ChPCOs treated with IMP-1088 or Apilimod exhibited significantly reduction in fewer SARS-CoV-2 infected cells (Figs. 2D, 2F)." I think the wording needs to be corrected here. A "reduction in fewer infected cells" sounds like an increase to me.
We thank the reviewer for picking up this mistake. We have now modified the sentence on Line 242: "All treatments, IMP1088, Apilimod, and Nafamostat, significantly reduced the number of infected cells compared to DMSO controls (Fig. 2E).".

5. Page 7: "In addition, Wwe also quantified the level of SARS-CoV-2 infection in ChPCOs using virions released from either DMSO or IMP-1088-treated cells (Fig. 2E)." Please correct the typo.
The typo has been corrected.

6. Suppl. Figure Legends refer to the organoids as CPCOs, whereas they are called ChCPOs in the test. Please unify the annotation.
The ChCPO annotation is used now throughout the paper.

7. Methods section (Page 7 of supplemental information): "Double detection was performed to …" Please correct the typo ("Doublet").
Typo has been corrected.

8. Page 9: "Following the findings of the mass sp 19ectrometry analysis". Please correct the positioning of the reference.
The unnecessary reference has now been removed from Line 330.

9. Page 10: "N-myristoylation is a conserved feature of ARFs, including ARF1[47]. To characterize the effects of IMP-1088 treatment on secretory pathway trafficking further, we next compared the of IMP-1088 treatment to Brefeldin-A (BFA), which is an ADP-ribosylation factor 1 (ARF1) inhibitor …" Please introduce the ARF abbreviation when using it for the first time.
We thank the Reviewer for picking up the error. The abbreviation "ADP-ribosylation factor 1 (ARF1)" was already introduced on Line 100, and we have now removed the redundant mention.

Reviewer #6 (Remarks to the Author):

The manuscript of Saber et al. focusses on the activity of IMP-1088, a drug that inhibits cellular N-myristoylation and was shown to have antiviral potential on Rhinoviruses. The drug is shown to inhibit SARS-CoV-2 infectivity by disrupting viral assembly and maturation thus releasing virions with compromised infectivity. The hypothesis put forward is that incomplete maturation in IMP-1088 treated cells is due to lack of Furin cleavage because virions are diverted from ERGIC/Golgi where Furin resides to lysosomes/plasma membrane. If the purpose of the manuscript is to describe the mode of action of an antiviral drug first would be necessary to convince the reader that the drug could be potentially effective in vivo. Cellular

models of infection included A549-AT cells, nasal epithelial cells and human 3D choroid plexus-cortical neuron organoids. However, cytotoxicity was measured only for A549-AT and also incompletely. Furthermore, the drug, which is almost an irreversible inhibitor of N-myristoylation, may impact essential activities that may not appear in a cytotoxicity assay in cell culture. Hence, the data provided so far are not yet sufficient to put too much emphasis on antiviral development. Some experiments such as: (lack of) inhibition of other viruses, scRNAseq, proteomic analysis are poorly contextualized in the logic frame of the work. The manuscript is written sometimes in a disordered way in the flow of experiments and would need to be better structured. The final model of altered secretion requires more evidence.

Specific comments:

1.Virus inhibition in A549-AT cells shows 50% efficacy at 24hpi and better effect at 48hpi (except for Omicron that remains at 50% inhibition also at 48hpi). Being such a potent inhibitor why it takes so much time for complete inhibition? In 24 you may have reconstitution of HMT activity from neo-synthesized protein.

Our results indicate that NMTs activity does not seem to recover during infection as shown by the drug-wash out experiments demonstrating similar antiviral profiles even when the drug was washed out after 1 min treatment (Fig. 4K-N; Fig. S1A-C). Thus, even if NMTs are inhibited quickly and nearly in irreversible manner, the effect on some cell functions is slow. Our interpretation of the delayed antiviral effect is now included in the Discussion Line 616: "Despite fast inhibition of NMTs (within one minute), the observed antiviral effect was progressive, starting after 12 h of treatment and reaching its maximal effect within 48 h. This slow effect suggests that the cellular proteins that are myristoylated before the drug treatment have a slow turn-over. Indeed, blocking NMTs has been shown to induce faster degradation specifically of NMTs targets, which we validated in the A549-AT cells used in our study.".

2.Cytotoxicity assay in A549-AT cells is not complete; it stops at 1 uM with already signs of toxic effect. A complete CC50 and EC50 profile with selective index would be welcome both at 24/48 hpi with the same protocol of exposure to the drug.

As requested, the cytotoxicity test was extended to 10 uM for IMP-1088 and these new results are now shown in Fig. S1D. We also assessed the combined effects of SARS-CoV-2 infection and drug-treatment on A549-AT cell viability (Fig. S1E). While 10 µM IMP1088 caused a significant decrease in A549-AT cell viability, the drug-treatment at 3.9 nM-1 µM had no cytotoxic effects on cells (Fig. S1D). The drug also did not induce further cytotoxic effects on infected cells (Fig. S1E). Therefore, the CC50 is not calculated.

We also assessed cell viability in human nasal epithelial cells derived from three adult donors and cultured under submerged conditions and treated with DMSO, 0.01-10 µM IMP1088 or 2.5 µM puromycin for 48 h. A modest donor-specific variation in response to 1 µM IMP1088 was observed, with one donor exhibiting a slight decrease in viability after 48 h of treatment, while the other two showed no effects to 1 µM treatment (Fig. S1F). In contrast, treatment with 10 µM IMP1088 or 2.5 µM puromycin resulted in a significant reduction or a decreased trend in viability across all donor samples (Fig. S1F).

In addition, a water-soluble NMT inhibitor IMP1320 showed significant efficacy in blocking SARS-CoV-2 infection in A549-AT cells (Fig. S4A, S4B) with no detectable cytotoxicity (Fig. S4C). IMP1320[50,51] and another NMT inhibitor PCLX-001[40], have been demonstrated to inhibit NMTs *in vivo*, with no overt toxicity. PCLX-001 is currently tested in a clinical trial for cancer[40].

EC50 values for IMP1088 and IMP1320 have now added into the Figures (Fig. 1C, 1D, 1F, and Fig. S4B).

3.A complete ToA (time of addition) experiment with addition of the drug at timepoints after infection and a virucidal activity on the virion would be a more comprehensive testing of an antiviral drug.
In the new experiments included in the paper (Fig. 4O, S4F, S4G), we show that the defect of the drug on the infection is detectable from 12 hpi onward. No difference in virus release (Fig. 4I, 4J) or viral RNA synthesis (Fig. 4D) was detected 8 hpi. In addition to demonstrations showing antiviral effects of IMP1088 when added before or after infection (such as Fig. 1C, 1D), and based on the above results, extensive ToA experiments were not performed.

4.Not clear the meaning 'sequencing the virus just after treatment'. Usually virus that overcomes drug inhibition is sequenced after passaging several times under drug selection. Here seems to be 24-48hpi, not clear, Table 1 is missing?
We apologise if our text was not clear. The aim of the experiment was not to test the potential development of drug resistance due to escape-mutations but rather to explain why the virion infectivity was compromised in IMP-1088 treated cells. Antiviral drugs such as molnupiravir cause an increase in the mutation rate of the viral polymerase resulting in the production of non-infectious virus mutants. To test this possibility, we sequenced the virions produced from cells treated with vehicle controls or IMP-1088 and observed no increase in mutations, thus excluding that the effect of the drug is due to an increase in mutation rates. This has now been clarified in the main text (Line 294) and discussion (Line 600). The results are included in Table 2.

5.The experiment at 8hpi figs 1H-j could be interpreted differently, being a drug acting fast on the cellular HMT enzyme but exerting its antiviral effect slow requiring 48-72h.
We agree with the reviewer and have modified the text to clarify that this is, indeed, our interpretation. In addition, to better exclude effects on virus entry due to short incubation times, we have added experiments where drug was added 24 h before infection, followed by SARS-CoV-2 Wuh infection for 6h (Fig. 4E). No effect on the early stages of infection were observed indicating that viruses can still enter, but the assembly and infectivity of progeny virions is compromised in cells where NMT activity is inhibited for sufficient times.

6.Nasal cells from human donors are quite heterogeneous depending on various factors including age, how many different donors per experiment?
We used cells from three adult donors. The results were consistent across all donors. The three donors are now indicated in the Methods, Figure legends and main text.

7. The experiment in nasal cells lead to a statement of defect in spread of the NMT inhibition without actual evidence of it, which comes later on in the text.

We thank the reviewer for pointing out this mistake. We have now clarified the text and say "Consistent with our findings in A549-AT cells, IMP1088-treatment strongly inhibited SARS-CoV-2 infection in human primary nasal epithelial cultures, while blocking virus entry by combined inhibition of TMPRSS2 using Nafamostat[35,36], and endosome maturation using Apilimod[37,38], resulted in a complete inhibition of infection (Fig. 1W).".

8.Testing different viruses would be useful to check for specificity of treatment and eventually to classify mechanism based on similar action. However, from the text it is not clear why they are doing this testing. What is the discriminant among these 4 viruses? Needs explanation/clarification.

To date, the antiviral activity of IMP1088 has been demonstrated against the common cold rhinovirus, vaccinia virus, and yellow fever virus which all harbour one or more proteins that undergo *N*-myristoylation. SARS-CoV-2, on the other hand, does not, based on current knowledge, have *N*-myristoylated proteins. To our knowledge, SFV, VSV and RSV also do not have *N*-myristoylated viral proteins. We have now clarified this on Line 154: " Next, we tested IMP1088 effects against Semliki Forest virus (SFV, family Togaviridae)30, Vesicular stomatitis virus (VSV, family Rhabdoviridae)31, and Respiratory syncytial virus (RSV, family Pneumoviridae)32, all of which, based on current knowledge, lack N-myristoylated viral proteins.".

9.Furthermore, Fig 1 panels P,Q,R, show 2 conditions 1 or 2 hbi pretreatment with drug and 24 or 48 hpi test of infection, what is the rationale? Not really comparable.

We thank the reviewer for this comment and have addressed these experiments in new experiments in the light of the comment 3 made by Reviewer 1 who inquired about the used MOIs.

To address the MOI, in short, viral replication kinetics vary by virus and cell type: VSV and SFV replicate rapidly (up to 10^9 infectious units/mL within 20 h), while SARS-CoV-2 and RSV replicate more slowly (10^6 infectious units/mL in 48 h). We performed extensive dilution series for each virus and selected MOIs that yielded comparable infection levels at 24 hpi (Fig. 1P). Note that SFV infection appears as GFP-positive puncta, whereas VSV infection results in uniform cytoplasmic GFP expression. To better compare the effects of IMP1088, we repeated the VSV and SFV infection experiments using MOI 0.001, which allows multiple rounds of infection over the 24-h experimental period. A549 cells were pre-treated with IMP1088 either 1 h or 24 h prior to infection and fixed after 24 h (extending infection to 48 h results in extensive cell death and detachment).

Unlike our earlier experiments with higher MOIs, the new data show that IMP1088-treatment 24 h prior to infection significantly inhibited VSV, but not SFV (Fig. 1R and 1S, respectively). While further studies are needed to understand why SFV is unaffected, we speculate (Discussion, Line 589) that the high spike density on SFV virions may compensate for partial loss of fusogenic activity following NMT inhibition. In contrast, SARS-CoV-2, RSV, and VSV have sparser surface spike densities, potentially making them more susceptible to spike impairments, leading to loss of infectivity.

In terms of the addition of the IMP1088 onto the A549 cells, we have now compared the effects of this NMT inhibition at 1.5 hbi for RSV, VSV and SFV. These experiments show that a pretreatment with IMP1088 inhibits RSV infection but does not have an effect on VSV and SFV infections (Fig. 1O-S). When we pretreated the A549 cells with IMP1088 at 24 hbi, the VSV infection was inhibited, but no effects were seen on SFV infection (Fig. 1R, 1S).

10. Is choroid plexus the right model to use? Neuronal infection of SARS-CoV-2 is highly debated and need to be more cautious on this. A model based on pulmonary cells would have been safer.

We thank the reviewer for this comment. We would like to clarify that the aim of the organoid experiments was to assess the role of NMTs in SARS-CoV-2 infection specifically in neurons. With our organoid models, the neuronal infection is readily observable without transgenic expression of virus entry factors (Fig. 2). We aimed to show that in the context of a neurons (would they ever be directly infected even at very low levels *in vivo*), the drug is effective. As a model for respiratory cells, we have primary nasal epithelial cells grown at Air-liquid interphase (Fig. 1T-W) and as submerged cultures (Fig. S1F), and we have now included experiments on Calu-3 cells (Fig.1 H-J). Although the extent of SARS-CoV-2 infection in the human brain is not clear, evidence indicating the presence of viral components in the brain tissue have been produced (PMID: 36517603). In the organoid model that we used, which includes neurons, immature astrocytes, and choroid plexus cells (PMID: 38838150; Fig. A, S2, S3), the observed neuronal infection was higher compared to previous models, averaging ~5% and exceeding 10% in cortical-like layers (PMID: 38838150; Fig. 2F). In contrast, SARS-CoV-2 infectivity in 2D and 3D neuronal models lacking a choroid plexus component has been consistently low -around 0.1% (PMID: 37039676, 38172412, 38749422, 37495586). Moreover, our recent work shows that SARS-CoV-2 spreads among neurons over 72 h in this model (Kettunen *et al*., bioRxiv preprint: https://doi.org/10.1101/2024.11.21.624622, in revision). Here, our data shows that IMP1088 efficiently inhibits viral infection and reduces the overall apoptotic index in organoids (Fig. 2G). This rationale has now been clarified in the main text relative to the experiments in organoids. We do not want to imply that SARS-CoV-2 is a virus to be considered bona fide neurotropic.

11. Concerning choroid plexus scRNA data, what is the relative composition of cell types infected by CoV2, need to show viral transcripts in the graph – here they also start to talk about decreased infectivity of released virions. This is reinforced in the next paragraph measuring infectivity of released virus.

First, we thank the reviewer for pointing out again that the order of experiments was not optimal. In the revised paper we have moved the experiments showing effect of the drug on virus release and infectivity after the ALI and organoids results.

Concerning the scRNAseq, we did not perform this technique in infected cells, but only in non-infected cells to characterize the model system. We have previously demonstrated that SARS-CoV-2 infects mainly the choroid-plexus epithelium, and a low number of neurons (PMID: 38838150), and here we colocalize infected cells with the neuronal marker MAP2 (Fig. 2F).

12. Page 8 – they state that "Following our findings of host cell NMT inhibition leading to a significant decrease in infectivity of the released virions and the perturbed trafficking of the viral particles to ERGIC and Golgi compartments, we next explored …." Where is the evidence? Again it comes later in the text.

We apologies for the mistake in the original version of the manuscript. The main text and conclusions now follow the data shown in figures.

13. Figure 3 (F) Western blot of uncleaved viral spike (S) ± glycosylation? Where is the evidence of glycosylation? Don't see different migration of bands.
We thank the reviewer for this comment. We have now included a new shorter exposure of the WB in Fig. 4P. It shows an additional band for virions released from DMSO-treated A549-AT cells, compared to virions released from IMP1088-treated cells. The longer exposure of the same WB is now included in Fig. S4L, showing that this extra band is undetectable in the NMT inhibited samples. These results suggest a possible difference in S glycosylation. We have now clarified this in the main text.

14. The mass spec data show info on perturbation of myroistilated proteins by the inhibitor. Some discussion would be required on other pathways such as activation of ER Stress pathways that could contribute to inhibitory phenotype.
We agree with the reviewer. In addition to the Gene Ontology (GO) pathway enrichment analysis shown in Fig. 5A and over-representation analysis (ORA) shown in Fig. S5C, the possible contribution of unfolded-protein response in the ER, extracellular matrix organization, posttranslational protein modification, post-translational glycosylation diseases, Golgi cisternae, lipophagy and COPI-dependent Golgi-ER trafficking are now presented as a heatmap in Fig. 5D. These results indicate that other pathways may have a role in the drug-induced anti-viral response of the host cells.

15. Electron microscopy shows gross rearrangement of membranes, IF shows disruption of ERGIC. Immunostain shows disruption again. All descriptive. All this part is in sterile (non infected) conditions and related to the function of the inhibitor. Functional data follow with ARF-GFP again in sterile(non infected) conditions. Any data in infection?
The quantitative data of non-infected cells, demonstrating the effect of IMP-1088-treatment on A549-AT cell ERGIC and Golgi, are shown in Fig. 5E-R and for ARF1 in Fig. S6. These results describe the effects of the drug on the secretory pathway in the absence of viral infection.

In addition, the quantitative data of infected cells, with colocalization of SARS-CoV-2 viral spike with endogenous ERGIC and Golgi are shown in Fig. 6C-F, and with endogenous LAMP1 in Fig. 7B. To investigate the viral egress in NMT inhibited cells, and to exclude the contribution of viral endocytosis, the egress is separately addressed using ectopically expressed SARS-CoV-2 viral spike, which is quantified for colocalization with endogenous markers LAMP1 (Fig. 7H) and calreticulin (Fig. 7L).

These experiments show how the combined effect of the drug and viral infection, each causing per se a strong alteration of the secretory pathways, results in differential localization of viral and cellular components in drug vs control treated infected cells.

Taken together, the results show that the drug treatment does not stop secretion of spike and virions but rather enhances it. However, the pathway of virus release is changed as suggested by the enhanced extracellular colocalization of the viral spike with ER and lysosomal luminal markers in IMP-1088 treated infected cells compared to vehicle controls.

16. Furin comes up as surprise next. What I the rationale?

We apologies if this part of the paper lacked sufficient background. To improve readability and better introduce the role of Furin, and rationale of the experiment, we have now added the following text in the introduction (Line 75): "Additionally, SARS-CoV-2 S proteins are further cleaved at a multibasic site into S1 and S2 subunits by the Golgi enzyme Furin, presumably in the trans-Golgi network (TGN)[10]. The virions initially bud into the lumen of the ERGIC, and are then released from the cells through a not fully characterized process that appears to involve transport through lysosomes, before calcium-dependent secretion[11,12]. The furin cleavage between the S1 and S2 domains of the spike is important because it 'primes' trimer for an early intermediate conformational change that occurs upon binding to ACE2 and exposes the second TMPRSS2-cleavage site, called S2', required for fusion[13].".

We have now moved the Furin results to Fig. 4T, to complement the experiments related to the viral proteins. We say in the main text (Line 383): "The reduced infectivity of progeny virions likely results from impaired assembly, characterized by decreased levels and defective Furin cleavage of the S protein. To assess whether reduced S protein cleavage contributed to the observed infectivity defect, SARS-CoV-2 Alpha virions released and collected from IMP1088–treated cells were treated with exogenous Furin. We then infected A549-AT cells with Furin-treated virions at the same I.U. for 48 h, fixed the cells and stained for N-protein. Quantification of relative infection showed that Furin-treatment significantly enhanced the infectivity of the virions released from IMP1088-treated cells but had no effect on those released from DMSO-treated controls (Fig. 4T). This supports the notion that impaired infectivity in IMP1088–treated cells at least partially results from a Golgi bypass and insufficient Furin-mediated processing of the S protein.".

In addition, we now have included results form our proteomics analysis, demonstrating that (Line 538) ".. Golgi-resident enzyme Furin[10], which was found significantly downregulated in our proteomic analysis following IMP1088–treatment (Table 3).".

We have also included our interpretation of these results in the Discussion (Line 627): "Thus, in NMT-inhibited cells, the maturing virions either do not meet active Furin efficiently, or they access a compartment where Furin is only partially active.

17. Fig 7A – seems that treatment did not decrease infectivity comparing the two graphs, but maybe two different dataset, explain.

The IMP1088 did have an effect similar to previous experiments presented in the paper but in this experiment, in each graph, the infection values were normalized to the levels obtained in the absence of Furin (indicated as 1). We think that normalizing the data better shows how addition of furin does not significantly increase infectivity of viruses released from DMSO-treated cells (because the spike is already cleaved by furin), however, it strongly increases the infectivity of virions collected from IMP1088 treated cells.

18. Final chapter deals with the Spike secretion using ectopic expression of S-wt, but the construct is not well described, is it full Spike with TM or w/o? Ancestral seq?

We have now added the description of the construct. We used the full-length spike of the Wuhan strain without any deletion. This is now mentioned in Methods.

19. What means “immunostained against internal (magenta) and secreted (green) Swt”

We apologies if the text here was not clear. We have now changed the text to improve readability Line 569: “To investigate this, A549-AT cells were transiently transfected with a plasmid that ectopically express SARS-CoV-2 S^{wt}, which, in the absence of other viral components, is retained in the secretory pathway (mainly ER and Golgi) and not secreted outside of the cells (Fig. 7F; note the perinuclear staining). 1 µM IMP1088-treatment for 48 h increased the secretion of the ectopic S^{wt}, which was detected outside of the cells (Fig. 7F, 7G), supporting the notion of an activation of Golgi-bypassing egress route following IMP1088-treatment. Pearson co-localization analysis of ectopically expressed S^{wt} against endogenous LAMP1 immunofluorescence staining increased significantly following IMP1088-treatment (Fig. 7H). Together, these results support viral egress from lysosomes.”. This is also now clarified in the respective Figure Legend 7F: “Representative immunofluorescence images of A549-AT transiently expressing ectopic SARS-CoV-2 spike protein (S^{wt}) treated with DMSO or 1 µM IMP1088 for 48 h, fixed and stained for secreted S^{wt} (green, anti-spike staining in non-permeabilized cells) and intracellular S^{wt} (magenta, anti-spike staining in permeabilized cells). Nuclei stained with DAPI (cyan). Arrow points to perinuclear localisation of S^{WT} with limited trafficking to the cell surface (arrowhead). (G) Corresponding quantification of mean fluorescence intensity (MFI) of ectopic secreted S^{wt} vs. intracellular S^{wt} normalized to nuclei, and (H) Pearson correlation coefficient of ectopic intracellular S^{wt} with endogenous LAMP1.”.

20. Last part rather confused and needs clarification. The conclusion that defect virus maturation in treated cells is due to lack of Furin cleavage because virions are diverted from ERGIC/Golgi where Furin resides to lysosomes/plasma membrane is poorly supported by the data. Pathway of ectopic Spike may well be different from virion.

To better support the results obtained with the ectopic spike, we have repeated the experiments with infectious viruses (new Fig. 7C-E). Taken together the results show that in the presence of IMP1088, in both ectopically expressing and infected cells, the spike protein colocalizes with endogenous lysosomal marker LAMP1 markers at the cell surface. In addition, in IMP1088-treated cells, we observed additional virus-containing membrane clusters resembling the ER, which appeared to fuse with the plasma membrane and form narrow tunnels for viral egress (Fig. 7I). Supporting this, electron tomography (ET) revealed a small opening between the ER lumen-harbouring SARS-CoV-2 virions and the plasma membrane (Fig. 7J). ER–plasma membrane fusion in IMP1088-treated A549-AT cells was also detected by immuno-EM using endogenous calreticulin as a marker (Fig. 7K). While Pearson co-localization analysis of ectopic S^{wt} with calreticulin remained unchanged upon IMP1088-treatment (Fig. 7L), the NMT inhibition led to increased extracellular secretion of endogenous calreticulin (Fig. 7M). Although the exact identity of the virion-containing membrane clusters (Fig. 7I) remains to be determined, these findings suggest that they include at least some ER-derived components. We have modified the title of the manuscript to “Inhibition of host N-myristoylation compromises the infectivity of SARS-CoV-2 due to Golgi-bypassing egress” in reflection of these findings.

21. Would it be possible to rescue inhibition by targeting Furin to this undescribed secretion pathway? Here there is need of more supporting evidence.

Targeting Furin to the ER, where the virions were observed in the IMP1088-treated cells, would result into an inactive enzyme because Furin requires maturation in Golgi (PMID: 31406574). Thus, this experiment was not performed. We have however modified our Discussion as to not overinterpret the results (Line 627): “Thus, in NMT-inhibited cells, the maturing virions either do not meet active Furin efficiently, or they access a compartment where Furin is only partially active.”. Our interpretation of the loss of virion infectivity released from NMT inhibited cells, is the combination of decreased spike incorporation in the virions, inefficient furin cleavage of the spike, and possibly altered glycosylation of viral structural S and M proteins.

REVIEWERS' COMMENTS

The senior authors would like to inform the reviewers that during the revision process we became aware that the data shown in Fig. 1b–g, Fig. 1k–n, Fig. 3b–f, Fig. 3l–n, Fig. 3u, Fig. 5e–f, Supplementary Fig. 4d–f, and Supplementary Fig. 5a, b, j were derived from $n \geq 3$ technical replicates. For this revision, all these experiments have been independently repeated, and the figures now present results from $N \geq 3$ biologically independent replicates. As a result, you may notice small differences within some panels; however, the findings from the original submission were reproducible and the overall biological conclusions remain unchanged. We apologize for this oversight. All original data are provided in the Source Data Files and will be deposited in public repositories upon acceptance of the manuscript.

Reviewer #1 (Remarks to the Author):
In the current version of the manuscript, Saber et al have addressed most, if not all, of the major comments suggested by the reviewers. The authors have improved the overall clarity of the manuscript and more clearly described the figures in the legends. While the hPSC-derived ChPCO experiments now adhere to ISSCR guidelines (using three independent hPSC lines), whether the ChPCO model is the most relevant model for this particular study is questionable. As SARS-CoV-2-induced encephalitis is highly rare and the IMP-1088 experiments rely on pre-treatment of ChPCOs, their translational potential remains unclear. However, the data on the antiviral activity of IMP-1088 and its mode of action are of interest to both the SARS-CoV-2 and broader virology field.
We thank the reviewer for this comment and agree that cases of SARS-CoV-2–induced encephalitis are rare. However, growing evidence indicates that the acute and long-term consequences of SARS-CoV-2 infection on brain health remain incompletely understood including persistent brain alterations and neurodegenerative processes following infection (e.g. Que *et al. Sci Rep* **15**, 26400 (2025) and Seo *et al. Nat Commun* **16**, 10552 (2025)). Therefore, we believe that proving antiviral candidates for SARS-CoV-2, future variants, and potentially other neurotropic viruses that may follow a similar assembly pathway, may have therapeutic relevance.

Accordingly, the aim of the experiments performed in the ChPCO model was not to model the incidence of encephalitis per se, but to assess whether IMP1088 treatment can prevent and suppress SARS-CoV-2 infection in a human brain-relevant system containing neurons, immature astrocytes, and choroid plexus cells. This model recapitulates key barrier functions and produces cerebrospinal fluid–like secretions, thereby providing a relevant platform to interrogate viral entry, persistence, and reinfection in neural cell types. Accordingly, these experiments were designed to demonstrate that IMP1088 treatment inhibits viral spreading in this model, including within neuronal populations.

We have moved the SARS-CoV-2 infection results in the brain organoids, including the scRNAseq results, in Extended Data Figures 1-3.

Reviewer #2 (Remarks to the Author):
I co-reviewed this manuscript with one of the reviewers who provided the listed reports. This is part of the Nature Communications initiative to facilitate training in peer review and to provide appropriate recognition for Early Career Researchers who co-review manuscripts.
Thank you for your contribution.

Reviewer #3 (Remarks to the Author):

The revised manuscript is improved by adding new results and rephrasing the text. However, the conclusions, especially the hypothesis (in the abstract) that “NMT1 inhibition triggers a novel Golgi-bypassing pathway for SARS-CoV-2 progeny virion egress”, are not fully supported. The authors also stated in the review response letter that “ Based on the current understanding of Coronavirus assembly and egress, the virions are believed to reach the Golgi compartment where the viral E, M, spike must be glycosylated and, in the case of SARS-CoV-2, the spike is cleaved by furin. From the Golgi compartment a transport mechanism to the lysosomes has been proposed, which in turn results in delivery of mature virions to secretory lysosomal vesicles that have a neutral pH” Please list the references (research articles, since many reviews proposed various pathways) supporting the Golgi to lysosome egress pathways of SARS-CoV-2.

Whereas previous models support virus egress via the classic secretory pathway (ER, ERGIC, and Golgi where the viral spike is cleaved by furin), recent evidence demonstrated that the final step of virus release is mediated by secretory lysosomes. References 7, 10, 15, 16 have been added to Manuscript Line 84. Our data indicate that following IMP1088 treatment, defective virions are released via a pathway that does not involve ERGIC or Golgi - Instead, the defective virions are released from ER to plasma membrane or ER to secretory lysosomes and from there to plasma membrane. This is supported by the defective furin cleavage in the released virions, leading to decreased infectivity, which was rescued by in vitro pretreatment with furin (Fig. 3t-u). In addition, following IMP1088 treatment, viral spike localisation within ERGIC and Golgi decreased (Fig. 5; EM and immunofluorescence co-localisation), while colocalization of the secreted spike with lysosomal marker LAMP1 increased (Fig. 6b-h). Further supporting direct release from ER, ER-plasma membrane openings were observed by EM and 3D-EM (Fig. 6i-j) and luminal marker of ER, calreticulin, could be detected at the outer side of the plasma membrane in IMP1088 treated cells (Fig. 6k-m).

In contrast, it is widely accepted that SARS-CoV-2 undergoes a Golgi-bypass unconventional pathway for release, which was first proposed in 2020 (PMID:33157038) and strengthened by different groups (PMID:33422265; PMID: 36563151; PMID:34995113). Recently, two different teams reported that BFA treatment inhibits SARS-CoV-2 assembly and secretion (PMID: 40540531; PMID: 40634337), which suggests ER to Golgi pathway is important for SARS-CoV-2 assembly/trafficking and challenges the Golgi-bypassing egress pathway. Therefore, the authors prefer Golgi-bypassing pathway for SARS-CoV-2 release, and it is not novel but a more widely accepted model. The authors should make it clearer about the SARS-CoV-2 egress pathway under normal conditions and under N-myristoylation inhibition.

We apologies that our interpretation of the results was not clear. Our results support the model where SARS-CoV-2 virions are trafficked and mature through secretory pathway organelles including ERGIC and Golgi, and egress at least partially via lysosomal intermediates at the final step. Following host NMT inhibition with IMP1088, membrane trafficking in secretory pathway is disrupted, leading to fragmentation of ERGIC and Golgi. SARS-CoV-2 virions trafficking and maturation is accordingly perturbed, whereby the virions do not reach ERGIC and Golgi compartments as explained above, and egress both from lysosomal and ER membrane cluster

compartments. We have clarified this in the main text (Lines 648-658) and included the references pointed out by the Reviewer (Lines 84).

The authors reasoned that " To our knowledge, isolation of SARS-CoV-2 intracellular and intact virions is, thus, not feasible." For example, in the paper mentioned above (PMID: 40540530), intracellular virion titer was measured for a short period of SARS-CoV-2 infection. Also, WB for released virions was done after PEG enrichment, not supporting "WB could not be performed at this early time point (12 hpi)".
We thank the reviewer for this comment and acknowledge the possibility to retrieve intracellular virions after cell lisys. Although measuring the infectivity of intracellular virions would complement our results, we believe that in the revised manuscript sufficient evidence has been provided to support the effectiveness and the mechanism of action of IMP1088 as an inhibitor of virus assembly and release. In particular, we monitored RNA synthesis from 2-48 hpi and detected the first defects at 8 hpi following IMP1088 treatment (Fig. 3h). We also show defects in infectivity of released virions at 12 hpi (Supplementary Data Fig. 5d).

In Figure 7C, in addition to Spike and LAMP1 colocalization analysis, co-staining of Spike and a Golgi marker would be strong evidence to support the authors' conclusion.
The quantitative localization analysis of Spike and Golgi markers requested by the reviewer were provided in Fig. 5c-f, i.e. Spike (S1+2) with ERGIC (ERGIC-53) and Golgi (GM130).

In the paper (PMID: 40634337), Arf1 plays an important role in SARS-CoV-2 assembly by directly interacting and facilitating the ERGIC accumulation of M protein. As loss of N-myristoylation in Arf1 disrupts its Golgi membrane association, and 1 uM IMP1088 treatment did not significantly alter Arf1 Golgi association, more discussion will be valuable.
We agree with the reviewer and apologise if our previous explanation was not unclear. We clarify here that in the Supplementary figure 7 f-i of our manuscript, inhibition of NMTs does lead to a gradual but significant fragmentation Arf1 fluorescent signal. However, unlike Brefeldin-A treatment, which rapidly and directedly inhibits Arf-1 (Supplementary Data Fig. 7a-d), IMP1088 selectively inhibits *N*-myristoylation of only newly synthesised NMT substrates and, hence, does not affect pre-existing *N*-myristoylated proteins. Thus, the inhibition of Arf1 function is slower compared to the effect Brefeldin A and thus not observable during the first hour of treatment (Supplementary Data Fig. 7e). The estimated turnover of existing *N*-myristoylated proteins is slow (approximately 1–3 days, PMID: 19782106). Accordingly, the effects of IMP1088 on the Golgi depend on the turnover of existing *N*-myristoylated Arf1 at the time of drug treatment rather than on direct inhibition of pre-existing *N*-myristoylated proteins. Consistent with this interpretation, we observe a fragmentation of Arf1 foci within 48 h of IPM1088 treatment (Supplementary Data Fig. 7f-i). We have clarified this interpretation on Manuscript Lines 499-525.

Reviewer #5 (Remarks to the Author):

Overall, I applaud the authors for adding a considerable amount of new data to address the majority of my previous comments in a satisfactory manner, and I acknowledge that the manuscript has improved as a result of the revisions. I appreciate the effort made to clarify various aspects of the work.

Thank you, we appreciate the comment.

That said, I would like to raise a general concern about the review process. I had the impression that the authors did not take sufficient steps to facilitate the reviewers' task. Most notably, the absence of tracked or highlighted changes in the revised manuscript made it unnecessarily difficult to assess what had been modified. While the authors added line numbers, they only used them to refer to changes in some answers. This added considerable effort to the re-evaluation and, in my view, does not align with best practices in scientific communication.
We apologise for this oversight and for the inconvenience. The manuscript underwent substantial revision, and the extensive tracked changes made the text difficult to follow. To improve readability, we therefore accepted all changes at one stage. In this revision, we have included the tracked changes for clarity, along with references to Line numbers.

In addition, my specific request for a GEO accession number was not adequately addressed. Although the authors mention that this information was provided to the editor, I did not receive it. Accessing such essential data should not be this cumbersome, particularly when it is necessary for a proper and complete review.
We are sorry if the reviewer was not provided with this information. This information was provided to the Editor; however, it may not have been visible to the reviewers. The scRNA-seq dataset has now been deposited, and the GEO accession number is provided in the Methods section.

Finally, I found that the presentation of certain materials—especially Table 3, which lists the top 50 marker genes per cell type—still requires improvement. In its current format, the table is not particularly readable, which diminishes its utility. A dot plot, as I previously suggested, would have been a much more effective and accessible way to present this information.
We thank the reviewer for the suggestion to visualise the top 50 marker genes per cell type in Table 3 (now Table 1). We would like to clarify that these markers were originally identified to support the cell type annotation, with the top markers computed for each cluster relative to all others.

To improve clarity and better link the marker genes to cluster identity, we have now included UMAP visualisations for each cluster alongside Table 1. In addition, to address the reviewer's request while maintaining interpretability, we generated two complementary dot plots: (i) a plot showing the top 5 marker genes per cell type, and (ii) a plot highlighting the key marker genes used for cluster annotation. These are now presented in Extended Data Fig. 1b and Fig. 1d.

We also explored visualising the top 5 markers per cluster (1st image below), and top 50 markers per cluster as suggested as suggested (2nd image below). However, this resulted in substantial overcrowding and reduced interpretability of the results. We therefore believe that the revised presentation provides a clearer and more accessible summary of the marker gene expression patterns while still capturing the key biological signals.

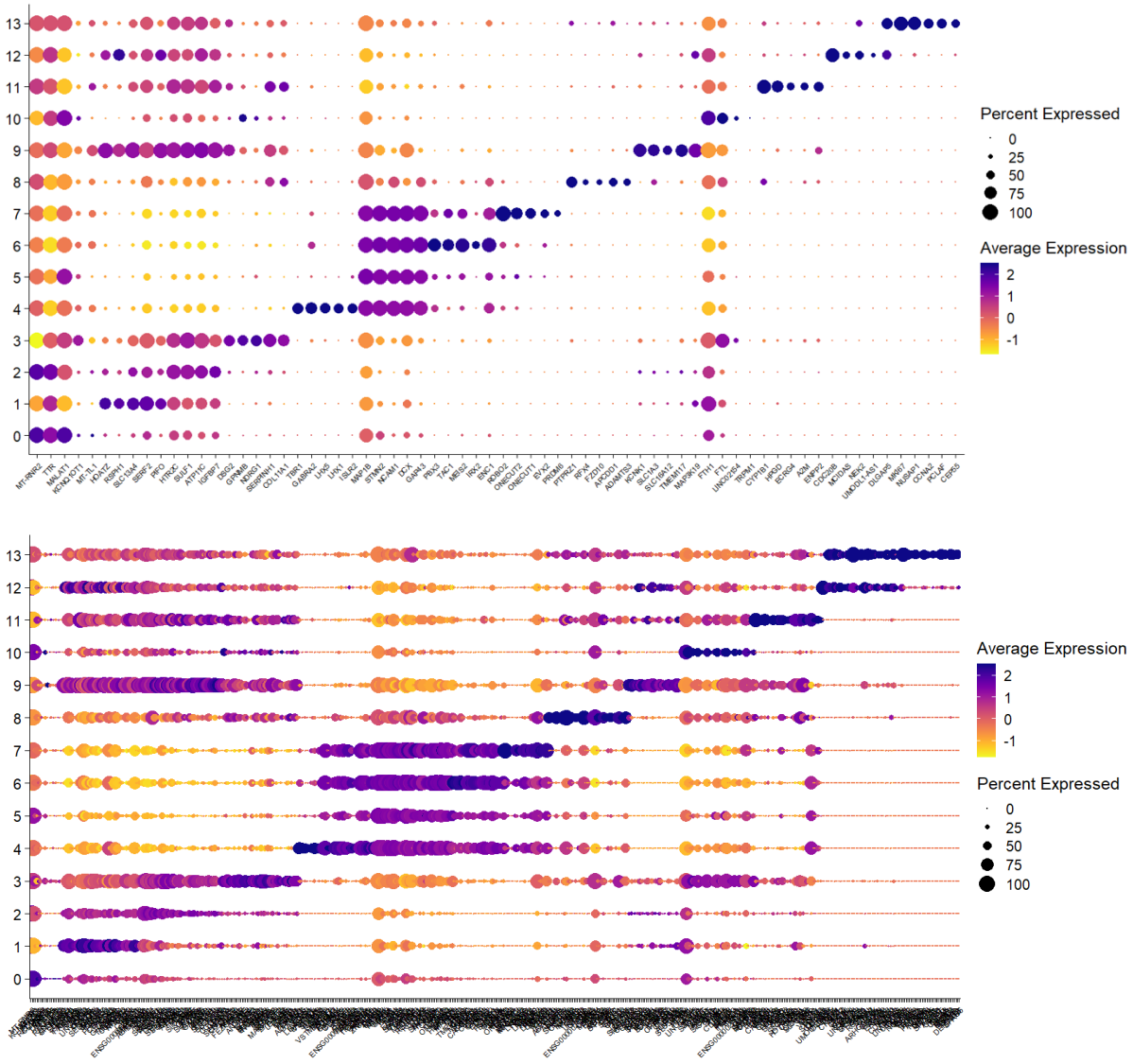

Nevertheless, I am convinced the paper will make a valuable contribution to the field, and I recommend accepting the manuscript for publication.
We thank the Reviewer for their recommendation.

Additional minor comments:

Line 76/77: "of" is missing.
We have corrected the typo.

Reviewer #6 (Remarks to the Author):
I'm happy with the rebuttal of the authors, manuscript is improved and could be published, no further comments.
We thank the Reviewer for their recommendation.